Bioactive Materials 7 (2022) 192–216

Contents lists available at ScienceDirect

Bioactive Materials

journal homepage: www.sciencedirect.com/journal/bioactive-materials

A review on current research status of the surface modification of Zn-based biodegradable metals

Wei Yuan [a], Dandan Xia [a,b], Shuilin Wu [c], Yufeng Zheng [a,b,*], Zhenpeng Guan [d,**], Julietta V. Rau [e,f,***]

[a] School of Materials Science and Engineering, Peking University, Beijing, 100871, China
[b] National Engineering Laboratory for Digital and Material Technology of Stomatology, National Clinical Research Center for Oral Diseases, Beijing Key Laboratory of Digital Stomatology, National Medical Products Administration Key Laboratory for Dental Materials, Research Center of Engineering and Technology for Digital Dentistry, Ministry of Health, Beijing, 100081, China
[c] School of Materials Science & Engineering, The Key Laboratory of Advanced Ceramics and Machining Technology by the Ministry of Education of China, Tianjin University, Tianjin, 300072, China
[d] Orthopedics Department, Peking University Shougang Hospital, No. 9 Jinyuanzhuang Rd, Shijingshan District, Beijing, 100144, China
[e] Istituto di Struttura della Materia, Consiglio Nazionale delle Ricerche (ISM-CNR), Via del Fosso del Cavaliere, 100-00133, Rome, Italy
[f] Sechenov First Moscow State Medical University, Institute of Pharmacy, Department of Analytical, Physical and Colloid Chemistry, Trubetskaya 8, build. 2, 119991, Moscow, Russia

ARTICLE INFO

Keywords:
Zn-based biodegradable metals
Surface modification
Corrosion behavior
Biocompatibility
Osseointegration

ABSTRACT

Recently, zinc and its alloys have been proposed as promising candidates for biodegradable metals (BMs), owning to their preferable corrosion behavior and acceptable biocompatibility in cardiovascular, bone and gastrointestinal environments, together with Mg-based and Fe-based BMs. However, there is the desire for surface treatment for Zn-based BMs to better control their biodegradation behavior. Firstly, the implantation of some Zn-based BMs in cardiovascular environment exhibited intimal activation with mild inflammation. Secondly, for orthopedic applications, the biodegradation rates of Zn-based BMs are relatively slow, resulting in a long-term retention after fulfilling their mission. Meanwhile, excessive Zn^{2+} release during degradation will cause *in vitro* cytotoxicity and *in vivo* delayed osseointegration. In this review, we firstly summarized the current surface modification methods of Zn-based alloys for the industrial applications. Then we comprehensively summarized the recent progress of biomedical bulk Zn-based BMs as well as the corresponding surface modification strategies. Last but not least, the future perspectives towards the design of surface bio-functionalized coatings on Zn-based BMs for orthopedic and cardiovascular applications were also briefly proposed.

1. Brief review on industrial Zn alloys and their surface modification methods

Date back to early 20th century, industrial Zn alloys were developed firstly and applied as a replacement for tin and lead alloys in pressure die casting of printing type [1]. Various alloying elements have been added into Zn to further optimize the performance. Among them, Al was regarded as an advantageous element in the initial stage. It can improve the fluidity of melt as well as the mechanical properties of alloys [2]. Hence, Zn–Al system has been developed as the basis of most commercial alloys in casting industries. In terms of industrial applications, Zn and its alloys have been widely used in the protection of steel against corrosion [3,4]. Almost half of the production of Zn comes into service for coatings [5]. Different methods have been adopted to prepare the Zn coatings including hot-dip galvanizing (HDG), electroplating, metalizing, mechanical plating and Zn rich paint [6]. Among them, HDG is considered as a specifically effective and efficient method for the application of Zn coatings due to its convenience and high cost performance. Since 1800, HDG technique has been confirmed as a feasible approach subsequent to the exploration of iron and zinc [6]. The process

Peer review under responsibility of KeAi Communications Co., Ltd.
* Corresponding author. School of Materials Science and Engineering, Peking University, Beijing 100871, China.
** Corresponding author. Orthopedics Department, Peking University Shougang Hospital, No. 9 Jinyuanzhuang Rd, Shijingshan District, Beijing, 100144, China.
*** Corresponding author. Istituto di Struttura della Materia, Consiglio Nazionale delle Ricerche (ISM-CNR), Via del Fosso del Cavaliere, 100-00133, Rome, Italy.
E-mail addresses: yfzheng@pku.edu.cn (Y. Zheng), guanzhenpeng@qq.com (Z. Guan), giulietta.rau@ism.cnr.it (J.V. Rau).

https://doi.org/10.1016/j.bioactmat.2021.05.018
Received 25 February 2021; Received in revised form 9 May 2021; Accepted 9 May 2021
Available online 12 June 2021

involves immersion of the steel in the melt Zn, resulting in a sufficient coverage of Zn coatings. The galvanized Zn coatings can protect the steel substrate from the attack of aggressive corrosion media as physical barriers [7]. On the on hand, Zn is able to interact with the atmospheric compounds and forms a layer of dense, adherent and protective film on the coating surface. On the other hand, Zn also retards the corrosion of substrate thanks to the cathodic protective nature [8]. Nonetheless, the galvanized Zn coatings are apt to be damaged under the condition of wet, industrial or marine environment [5]. Meanwhile, note that the galvanized steel is usually painted, pretreatment is generally required for a better adhesion promoter [9]. Therefore, many attempts have been made to optimize the constituents of Zn coatings and improve the lifetime of Zn coatings. Alloying Zn with other elements such as Co, Ni, Fe and Mn can be an efficient way to further improve the protective effect of Zn coatings [10–12]. Besides, surface modification has also been adopted to improve the corrosion resistance of Zn coatings, mainly including chemical conversion coatings and organic coatings. The representative surface modification methods of Zn-based alloys for industrial applications are illustrated in Fig. 1.

1.1. Chemical conversion coatings

The formation of chemical conversion coatings involves a complex process of metal dissolution and precipitation, which usually proceeds in the aqueous solution [21]. The treatment is aimed at replacement of the native oxide layer of less corrosion resistance [22]. Chemical conversion coatings consist of the mixtures of different metal oxides and hydroxides dependent on the dissolved ions in the bath solution besides the zinc oxides and hydroxides [23]. Such conversion coatings can achieve tight adherence to the substrate due to the nature of chemical bonding as well as an improved corrosion resistance.

(1) Chromate conversion coatings

The chromate-based coatings have been widely used for the improvement of the corrosion resistance of metals as well as the adhesion of paints and lacquers in industrial system [13]. The formation of chromate conversion coatings involves a series of complex reactions [24]. The fundamental process can be summarized as the redox reaction between Zn matrix and Cr(VI) ions in the bath solution [24]. At the initial stage, Zn dissolves into Zn^{2+} in the acid treatment solution. Subsequently, the precipitation of Cr(III) forms and adheres on the surface, which is associated with the local pH increase attributed to the consumption of hydrogen ions during the reduction of Cr(VI). At the end, a conversion coating consisting of zinc oxides and hydroxides, zinc chromate, mixed Cr(III) and Cr(VI) oxides and hydroxides would be generated on the surface [25]. The insoluble components of chromate conversion coatings can effectively protect the substrate from the corrosion medium as physical barriers [13]. In addition, the chromate conversion coatings are also claimed to provide self-healing ability to metallic substrate under the circumstance of defect or failure. The water-soluble Cr(VI)-containing components in the coatings are able to migrate to the position of scratch and defect, where they would be reduced to form a passivation layer. Under this condition, the amount of the soluble Cr(VI) species which are absorbed onto or exist within the coatings after the chromating treatment plays a significant role in the corrosion protection [13,26,27].

Nevertheless, it is claimed that Cr(VI) chemicals used in the conversion treatment are toxic and carcinogenic [13]. Hence, much attention has been focused on the development of non-chromate passivation treatments. Cr(III)-based conversion coatings have been put forward as potential alternatives to the Cr(VI)-based conversion coatings on account of their comparable corrosion resistance but better biocompatibility [28]. Meanwhile, the preparation process of Cr(III) conversion coatings is similar to that of chromate counterpart in the industries [29]. The corrosion resistance of Cr(III) conversion coating, fabricated in the treatment solution containing nitrate as an oxidant and sodium

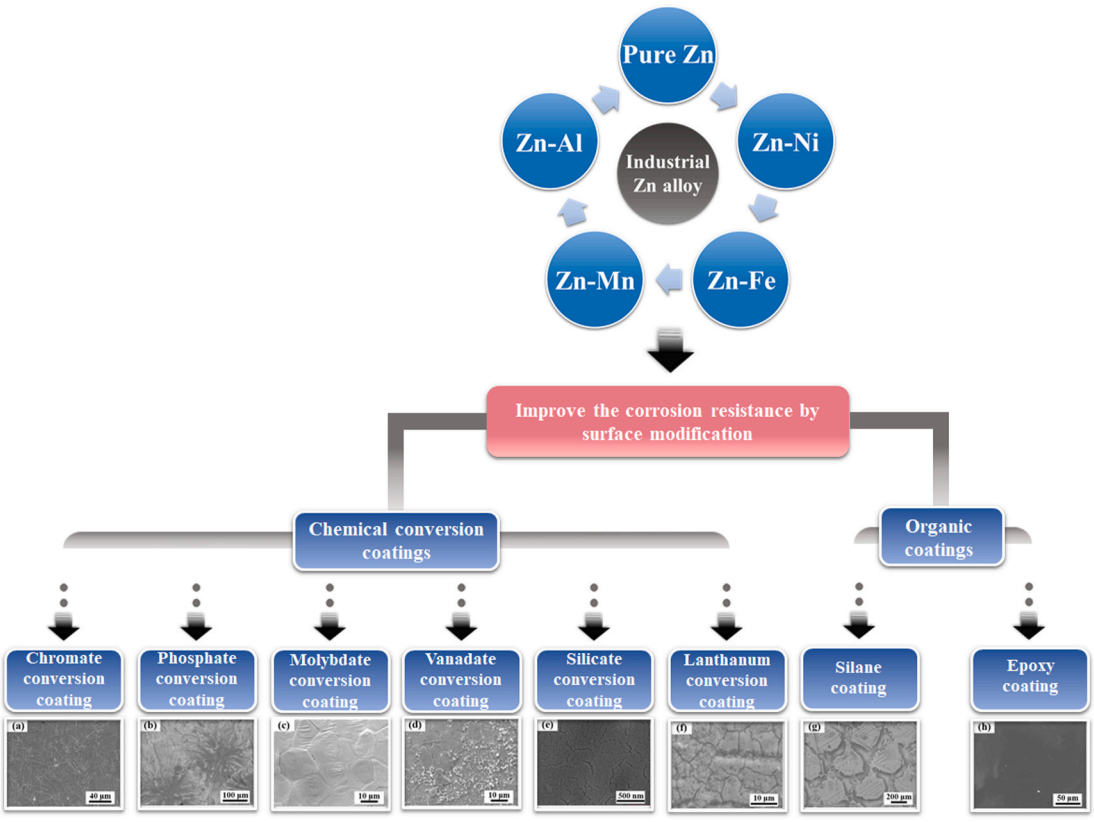

Fig. 1. The representative surface modification methods of industrial Zn-based alloys. (Reproduced with permissions from Refs. [13–20]).

hypophosphite as a complexant for the sake of the stability of Cr(III), was proved to be as good as chromated coating [30]. Bellezze et al. [31] claimed that the Cr(III) conversion coating exhibited improved corrosion resistance after immersion in Si-based solution for sealing treatment. It is also reported that the addition of transition metal ions such as Co(II), Ni(II) and Fe(II) into the treatment solution can further improve the corrosion resistance of trivalent chromate conversion coatings [32,33]. Nonetheless, the Cr(III) conversion coatings lack for the self-healing property in case of coating defect compared with the chromate coatings [29].

(2) Phosphate conversion coatings

The Zn phosphating is one of the most commonly used chemical conversion process to improve the surface properties, such as the corrosion resistance, wear reduction and adhesion for painting in industries [34]. Generally, phosphating treatment is conducted in acid phosphate aqueous solutions containing Zn^{2+} and $H_2PO_4^-$ as well as NO_2^- and NO_3^- as accelerators [35]. The phosphating reaction begins with the dissolution of Zn and air-formed oxide/hydroxide film upon immersion in the acid bath. Subsequently, the protons are reduced and consumed, resulting in the local pH increase near the Zn electrode surface. Meanwhile, pH increase promotes the dissociation of $H_2PO_4^-$ and HPO_4^{2-}. Thereafter, hopeite, the major component of the corrosion protection layer, deposits on the surface once the local pH is high enough [14]. The crystalline phosphate salts continue growing and cover the whole surface until being stopped by self-inhibition [36]. Although the hopeite crystals adhere well on the Zn-coated surface, irregular crystal shape results in the presence of open pores, which make it accessible for the corrosion attack [37]. In this way, the corrosion resistance of phosphate conversion coating is directly related to the coating porosity. Many efforts have been made to optimize the structure of phosphate crystals, decrease the grain size and improve the coating coverage. It is reported that pretreatment with colloidal titanium phosphate solution can increase the nucleation sites of hopeite during Zn phosphating [36,38,39]. In addition, incorporation of additives in the treatment solution, such as Mg^{2+} [40,41], Ni^{2+} [35,42,43] and Mn^{2+} [44], can also decrease the coating porosity and improve the corrosion resistance. Tsai et al. [40] reported that addition of Mg^{2+} into phosphate solution reduced the phosphate grain size and increased population density of grains, resulting in better corrosion protection. The same grain refinement effect of Mg^{2+} has also been reported by Ishizuka et al. [41] The incorporation of Ni^{2+} can modify the nucleation and growth rate of phosphate crystals in addition to the formation of Zn–Ni alloy on the bottom of pores [35]. Besides, silicate post-treatment can seal the pores in the phosphate conversion coatings and form continuous composite coatings, leading to increased corrosion resistance [45]. Lin et al. [46] demonstrated that post-treatment with molybdate solution was able to form dense and complete composite coatings on the surface, inhibiting both the anodic and cathodic process of Zn corrosion.

(3) Molybdate conversion coatings

Molybdenum, presented as an additive in electrolyte or alloying element, can effectively inhibit the corrosion of metals such as aluminum, zinc and steel as an environmental-friendly and effective corrosion inhibitor [47–50]. Molybdate conversion coatings have also been put forward as an efficient method to improve the corrosion protection due to their low toxicity. Molybdate-based passive films can be generated by immersion or with applied cathodic potential [15,51]. Generally, the protective effect of the conversion coatings rest on the coating thickness and compactness [15]. However, the molybdate conversion coatings are generally characterized by cracked “dried riverbed” morphology [52]. It is reported that the pH value of the treatment solution and applied acid used to adjust pH value play a significant role in the coating quality. The prepared film can provide a superior protection when the pH values range from 1 to 6 for any acid [53]. Magalhães et al. [53] demonstrated that Zn electrodes treated in the molybdate bath acidified with phosphoric acid exhibited better corrosion protection compared with those acidified with sulfuric acid and nitric acid.

(4) Vanadate conversion coatings

Vanadates have been considered as effective corrosion inhibitors to suppress the corrosion of Zn in aqueous solution [54,55]. Meanwhile, vanadate conversion coatings have been widely applied on the surface of Zn or HGD steel for the sake of corrosion protection [56–58]. It is claimed that the corrosion inhibitory effect is possibly attributed to the existence of the +4/+5 mixed oxidation state of the conversion coatings [59]. Zou et al. [16] constructed vanadium conversion coating, which is mainly composed of closely packed particles of V_2O_5, VO_2 and their hydrates on the surface of electrogalvanized steel. They found superior corrosion resistance of vanadate-treated samples compared with that of untreated and chromate-treated samples.

(5) Rare earth metal salts conversion coatings

Rare earth (RE) salts have been proposed as promising corrosion inhibitors on a variety of metals [60–63]. It is reported that rare earth compounds can improve the corrosion resistance of metals by constructing a layer of protection film on the metallic surface [64–66]. Local alkaline environment by reason of oxygen reduction leads to the precipitation of RE oxides/hydroxides on the cathodic areas of metals [67–69]. The immersion of Zn in the aqueous solution of $Ce(NO_3)_3$ is able to form a layer of passive film mainly consisting of oxides and hydroxides of Ce(III) and Ce(IV) [66]. Meanwhile, cerium conversion coating modified with $Ce(NO_3)_3{\cdot}6H_2O$ exhibited favorable self-sealing property [70]. Ce^{3+} in the coating can migrate to the scratch and cover the damaged sites with the precipitation of $Ce(OH)_3$ or Ce_2O_3. Zhang et al. [71] reported that the lanthanum salt conversion coating, mainly composed of $La(OH)_3/La_2O_3$ and $Zn(OH)_2/ZnO$, was prepared on the surface of HDG steel, resulting in improved corrosion resistance. Montemor et al. [69] compared the effects of different RE conversion coatings on galvanized steel by immersion in the nitrate solutions of RE metals (cerium, yttrium and lanthanum). Although all the conversion coatings exhibited beneficial effects, the coating fabricated in the lanthanum nitrate solution showed the best corrosion protection. Moreover, modifying the rare earth conversion coatings with organic and inorganic inhibitors can further improve the protection performance of coatings. Gang et al. [72] demonstrated better corrosion resistance of lanthanum salt conversion coating when modified with citric acid.

(6) Silicate conversion coatings

On account of its superior inhibitory effect and high cost-effectiveness, sodium silicate is well known as the inhibitor and passivator to retard the corrosion process of metals [50,73]. Meanwhile, many researches have proposed silicate and silica as environmental-friendly and corrosion-resistant coatings on galvanized steel [17,74–77]. Yuan et al. [78] constructed silicate conversion coatings on HDG steel in a sodium silicate solution with SiO_2:Na_2O molar ratio ranging from 1.00 to 4.00. The conversion coating fabricated with a molar ratio of 3.50 showed the optimum corrosion resistance with more compact and uniform structure. Jamali et al. [79] deposited nano-silica potassium silicate conversion coatings on HDG steel. They found that the silica nanoparticles can fill the pores among the potassium silicate coating due to the fine particle size, giving rise to the improvement of corrosion resistance. In addition, it is reported that the silicate conversion coatings on HDG were featured by the favorable self-healing ability after immersion in sodium silicate solutions with SiO_2:Na_2O molar ratio of 1.00 and 3.50 [27]. The silicate anions in the

coatings can migrate to the scratched area and form a new layer of conversion coating. Nevertheless, the preparation of water-resistant silicate coating requires a high-temperature drying process in order to increase the corrosion resistance [80]. It is difficult to apply such post-thermal treatment in terms of large metals of irregular shape. Min et al. [17] claimed that the addition of potassium methyl siliconate into silicate conversion coating can improve the corrosion resistance without the need for thermal treatment.

1.2. Organic coatings

Organic coatings such as silane [19,81–87], acrylate [88] and epoxy resin [3,20] have emerged as promising alternatives. Among these, silane treatment is able to form a compact self-assembled silicon and oxygen network on the surface of metals. The resulting silane coatings are homogeneous and robust with superior corrosion resistance as physical barriers [89,90]. Chang et al. [81] fabricated silane coating on HDG steel by a sol-gel roll coating method and achieved improved oxidation and corrosion resistance. However, there were some small defects like pinholes or cracks in the coating, which were prone to be attacked by the corrosion medium. Therefore, additives including oxide nanoparticles [19,82–85] and ions [86,87] were incorporated into the silane matrix to improve the barrier and self-healing effects. Liu et al. [91] prepared a superhydrophobic coating with contact angle of 151 ± 2° on Zn by immersion into a methanol solution of hydrolyzed 1*H*,1*H*,2*H*,2*H*-perfluorooctyltrichlorosilane. The superhydrophobic coating displayed superior corrosion protection when immersed in 3% NaCl aqueous solution for 29 days.

A waterborne acrylic coating incorporated with titanium dioxide nanoparticles was fabricated on the surface of HDG steel by Lewis [88]. It was observed that addition of titanium oxide nanoparticles improved the protective effect of the coating due to its nature of hygroscopicity and high specific surface area.

Kartsonakis et al. [20] investigated the epoxy coating on HDG steel via dip coating process and demonstrated a promotional impact on the corrosion resistance as well as self-healing property. In addition, they also found that the addition of cerium molybdate nanocontainers loaded with corrosion inhibitor 2-mercaptobenzothiazole can further improve the corrosion resistance. Bajat et al. [3] claimed an increase in dry and wet adhesion strength of epoxy coating on HDG steel after pretreatment in hot air.

2. Current research status on biomedical Zn-based biodegradable metals

Commonly used metallic implants for biomedical applications are mostly made of stainless steel, titanium alloys and cobalt-chromium alloys. They possess excellent corrosion resistance and superior mechanical properties, maintaining a long-term mechanical stability *in vivo*. However, serious concerns still remain due to their non-biodegradability. Second surgery is necessary to remove the implants after the injured tissue healing, resulting in increased healthcare cost and further morbidity of patients [92,93]. In the past decades, biodegradable metals (BMs) have attracted much attention as temporary implants. In contrast to the traditional metallic biomaterials, BMs are mainly composed of essential metallic elements present in the human body in trace amounts. After fulfilling the mission of assisting tissue healing, BMs are able to gradually corrode in physiological environment with appropriate host response elicited by the degradation products [94]. In the design of biodegradable metallic implants, different parameters should be comprehensively considered to ensure their desired performance. Some specific design constraints and criteria for biodegradable implants based on the current research are displayed in Table 1 [95]. On account of these updated requirements, new challenges have been put forward in the development of BMs. Firstly, degradation products will be released into the surrounding physiological environment along with the proceeding of corrosion process (Fig. 2a). Although the BMs mainly consist of human essential elements, the concentration of released degradation products should be optimized to ensure their biosafety. Secondly, the degradation behavior of BMs should match the evolution and kinetics of the tissue healing process. As for the cardiovascular applications, the wound healing process includes three characteristic stages: inflammation, granulation and remodeling (Fig. 2b) [96]. A complete degradation of stent is expected after the vessel remodeling phase, prior to which the mechanical performance of stent should maintain stable (Fig. 2c). Besides, the fractured bone healing proceeds in three distinct stages: inflammation, repair and remodeling phases (Fig. 2d and e). In terms of different implantation sites, the healing periods of the specific injured tissues are varied, coming up with customized requirements for the degradation period of BMs (Fig. 2f).

Table 1
General design constraints and criteria for biodegradable metallic device applications (Reproduced with permissions from Ref. [95]).

Criterion	Cardiovascular stent	Orthopedic internal fixation device
Biocompatibility	Non-toxic, non-inflammatory, hypoallergenic No harmful release or retention of particulates Promote endothelial cell attachment; discourage smooth muscle cell attachment	Non-toxic, non-inflammatory, hypoallergenic No harmful release or retention of particulates Promote osteoblast and osteoclast attachment; avoid fibrous encapsulation
Mechanical integrity and resorption during service	Mechanical integrity: 3–6 months Full absorption in 1–2 years	Mechanical integrity: Plates and screws <6 months Osteotomy staples <3 months Full absorption in 1–2 years
Mechanical properties	Yield strength >200 MPa Tensile strength > 300 MPa Elongation of failure > 15–18% Elastic recoil on expansion < 4%	Yield strength >230 MPa Tensile strength >300 MPa Elongation to failure >15–18% Elastic modulus approximates to that of cortical bone (10–20 GPa)
Corrosion behavior	Penetration rate < 20 μm $year^{-1}$ Hydrogen evolution < 10 μL $cm^{-2} \cdot day^{-1}$	Plates and screws (0.5 mm $year^{-1}$) Hydrogen evolution < 10 μL $cm^{-2} \cdot day^{-1}$

So far, there are mainly three kinds of widely-investigated BM systems, namely Mg-based BMs, Fe-based BMs and Zn-based BMs. For decades, Mg- and Fe-based metals and alloys have been the research hotspots in the field of BMs. However, the rapid degradation of Mg-based BMs in physiological environment hinders their further clinical applications. Given the uncontrollable corrosion behavior, excessive release of degradation products as well as premature loss of structural integrity can bring about undesired host response after the implantation of Mg-based BMs [101–103]. In addition, the mechanical properties of Mg-based BMs are not strong enough for the load-bearing applications [104]. In contrast, Fe-based BMs are characterized by the superior corrosion resistance and mechanical properties. Nonetheless, the slow corrosion may lead to a long-term existence of implant *in vivo* [105]. Meanwhile, the corrosion products of Fe are claimed to be stable and accumulate for a long time *in vivo*, impairing the integrity of arterial wall [106].

Recently, much interest has been focused on the research of Zn-based BMs. With the intermediate standard electrode potential between Mg (−0.23 V_{SHE}) and Fe (−0.44 V_{SHE}), Zn (−0.76 V_{SHE}) has been put forward as a new research direction of BMs [107]. The preferable degradation behavior of Zn-based BMs is expected to match the healing

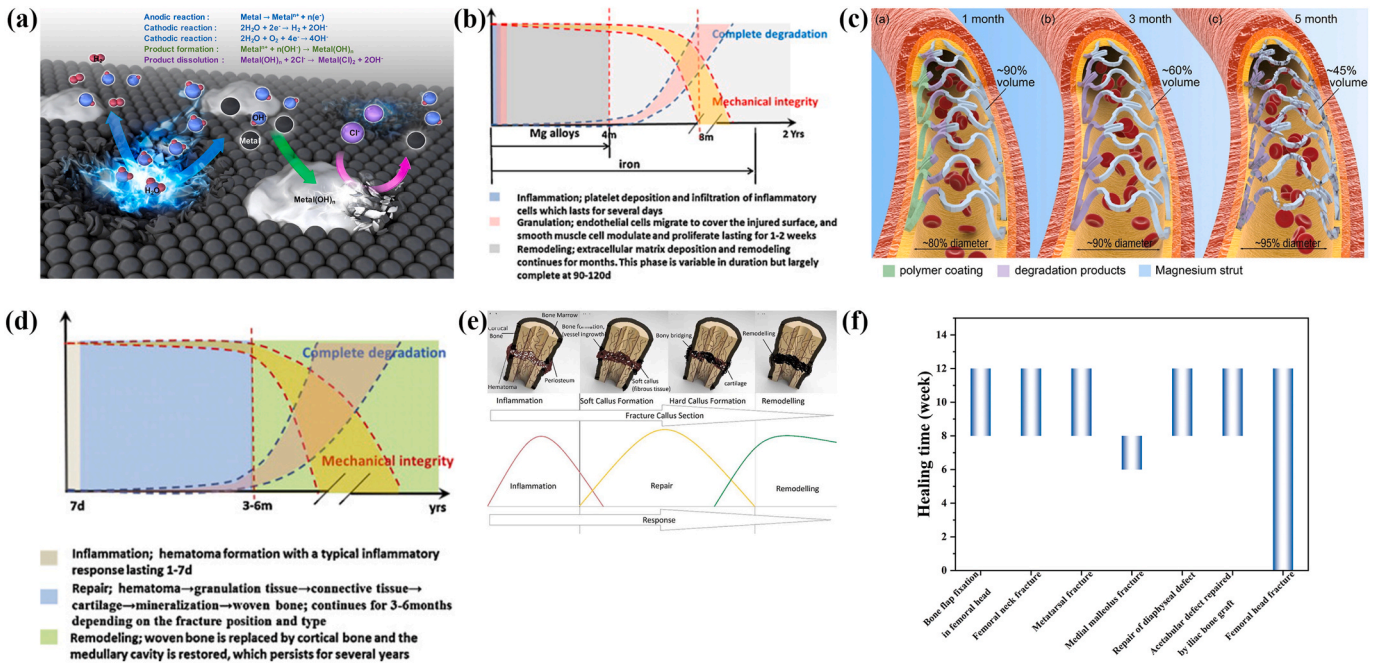

Fig. 2. (a) Biodegradation mechanism of metals. (Reproduced with permissions from Ref. [97]). (b) The evolution of degradation behavior and mechanical integrity of biodegradable metallic stents during the vascular healing process. (Reproduced with permissions from Ref. [94]). (c) Schema of biodegradable metallic stents over time post-procedure (The left part of the stent in each panel shows the surface layer and right part refers to the internal strut). (Reproduced with permissions from Ref. [98]). (d) The evolution of the degradation behavior and the mechanical integrity of BMs during bone healing process. (Reproduced with permissions from Ref. [94]). (e) Healing process stages in fractured bone. (Reproduced with permissions from Ref. [99]). (f) Healing period for the fixation of autologous bone grafts or bone fracture. (Reproduced with permissions from Ref. [100]).

process of injured tissue, meeting the standards of clinical applications. Besides, the mechanical strength of Zn-based BMs is superior to that of Mg-based BMs, suggesting their potential applications at load-bearing sites [108]. Meanwhile, it is claimed that the primary cathodic reaction is supposed to be the oxygen reduction during the degradation of Zn in neutral physiological environment, avoiding the accumulation of hydrogen gas [109]. The maiden attempt of Zn-based BMs for biomedical applications can be traced to 2007 by Wang et al. [110]. They designed Zn–Mg alloys with Mg content ranging from 35 to 45 wt% and evaluated the mechanical properties and corrosion behavior in simulated body fluid (SBF) solution. Thereafter, the *in vivo* research of Zn-based BMs was firstly investigated in 2013 by implanting the pure Zn wires into the abdominal aorta of adult male Sprague-Dawley rats [111]. The *in vivo* outcomes indicated the promising corrosion behavior of Zn-based BMs. From then on, developing novel Zn-based BMs including Zn-based alloys and composites have burst forth.

2.1. *The physiological functions of element Zn*

Zn is one of the most abundant transition metal ions in the body, second only to iron. In terms of Zn distribution in human body, 85% is present in muscle and bone, 11% in the skin and liver and the residue in other tissues [112]. The major absorption and excretion routine of Zn take place in the intestine. The existence of Zn has been demonstrated in

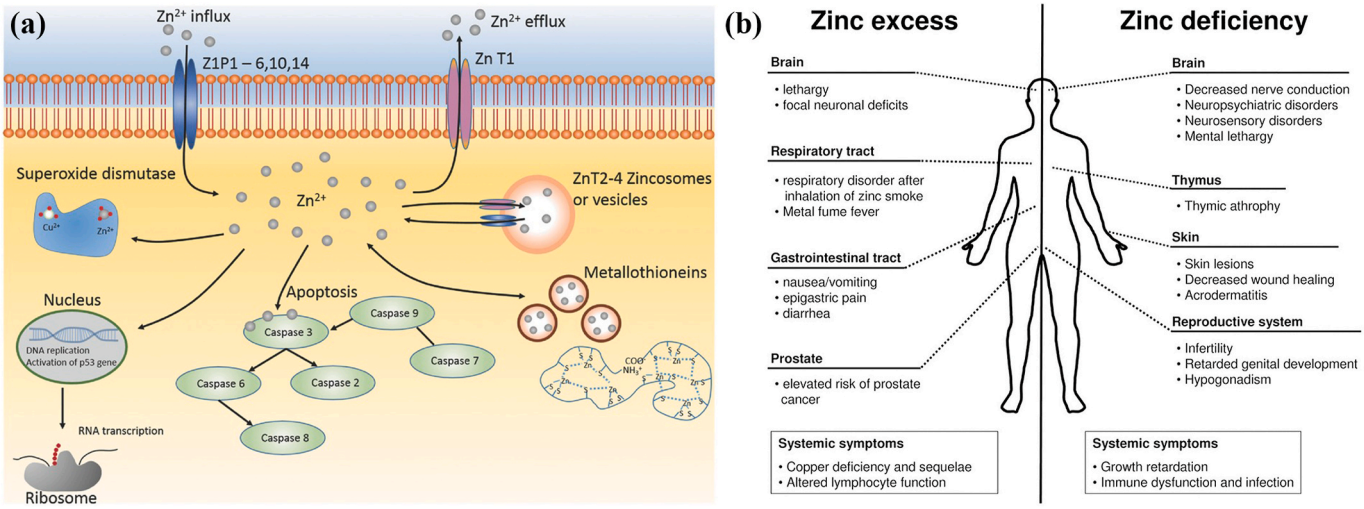

Fig. 3. (a) Biological roles of Zn. (Reproduced with permissions from Ref. [114]). (b) Comparison of the influence of zinc excess versus deficiency. (Reproduced with permissions from Ref. [131]).

more than 300 enzymes participating in their structure, catalytic and regulatory actions [113]. Zn plays a significant role in various biological functions [114] (Fig. 3a). It is indispensable for the growth of human and animals. Zn deficiency under different circumstance is directly associated with the retardation of bone growth, development and maintenance of bone health [115–117]. Both *in vitro* and *in vivo* studies have indicated that Zn can stimulate bone formation and mineralization [118,119]. Zn also interacts with vial hormones related to bone growth [120]. Incorporation of Zn into biomaterials is able to improve the osteoblast differentiation by promoting the bone marker genes such as alkaline phosphatase, collagen type I, osteocalcin and osteopontin [116]. On the other hand, in comparison with other metal cations, Zn is unique as a potent inhibitor of osteoclastic bone resorption with an apparent inhibitory effect at a concentration as low as 10^{-14} M [121]. Besides, Zn plays an important role in the protection of coronary artery disease and cardiomyopathy [122]. Supplement with Zn is able to improve the cardiac function and prevents further damage under the condition of ischemia and infarction [122]. Zn is important to maintain the normal endothelial integrity [123]. In addition, it can also stimulate the proliferation of endothelial cells by amplifying the endogenous basic fibroblast growth factor-dependent proliferation [124]. Zn is also associated with the development and integrity of the immune system. Zn has an important impact on the activity of some key immunity mediators consisting of enzymes, thymic peptides and cytokines [125]. Meanwhile, Zn is essential for intracellular regulation of lymphocyte apoptosis [125]. In addition, Zn participates in neurogenesis, synaptogenesis, neuronal growth and neurotransmission [126]. It is selectively stored in the presynaptic vesicles of specific neurons and released as neuro-modulator [126,127].

Although Zn is critical in plenty of physiological functions, excessive Zn exposure or intake can also result in detrimental impact on different organs in addition to insufficient Zn intake (Fig. 3b) [113]. Zn deficiency can result in a variety of pathological symptoms including growth failure, impaired parturition, hypotension et al. [112]. Many diseases are also accompanied by the lack of Zn such as gastrointestinal disorders, renal disease, sickle cell anemia and so on [113]. In contrast, excessive Zn can cause adverse consequence as well. Zn^{2+} is able to inhibit the electron transport in uncoupled mitochondria [128]. It is teratogenic or lethal for embryogenesis under the circumstance of excessive Zn intake [126]. Meanwhile, it is reported that Zn^{2+} has a biphasic effect on the cell viability, adhesion and proliferation. High concentration of Zn^{2+} would resulted in suppressive impact on cytocompatibility [129,130].

2.2. *In vitro and in vivo degradation behavior and biocompatibility studies on Zn-based BMs for orthopedic applications*

Recently, much attention has been paid to the applications of Zn-based alloys as orthopedic implant materials due to their preferable corrosion behavior *in vivo* as well as significant physiological functions of Zn ion [111,132]. The number of publications concerning Zn-based BMs for orthopedic applications since 2017 is 85 when analyzed via Web of Science database with the topics of Zn alloy and bone. Nonetheless, in view of the potential toxicity of Al, most commercial Zn alloys are not available for the biomedical applications [133,134]. Therefore, numerous researches have been carried out on the development of biomedical Zn-based alloys with the addition of human nutritional elements such as Ca, Mg, Sr, Mn, Li and so on [109]. However, the biosafety of Zn-based bulk materials still remains concerns due to the low inhibitory concentration threshold values of Zn^{2+} to cell and tissue [108]. The *in vitro* cytotoxicity and *in vivo* delayed osseointegration caused by the excessive release of Zn ions during degradation should be optimized for the further development of Zn-based BMs as orthopedic implants [135]. After implantation of Zn-based BMs *in vivo*, the corrosion products will gradually release into the surrounding physiological environment and react with the peripheral tissues and cells. The interactions between corrosion products and tissues at cellular and molecular level will influence a variety of physiological responses. The systemic investigation of *in vitro* and *in vivo* biocompatibility of Zn-based BMs have been conducted for orthopedic implants.

The *in vitro* cytocompatibility of recently reported Zn-based BMs for orthopedic applications is summarized in Fig. 4. Up to now, a number of *in vitro* cytocompatibility studies have implied that high concentration of the released Zn ions during the degradation process may cause cytotoxicity to osteoblast-like cells and fibroblasts. Su et al. [136] found a detrimental effect of 100% pure Zn extract on the cell proliferation and differentiation of MC3T3-E1 cell. Meanwhile, cells presented a round shape and limited spreading on the surface of pure Zn. Similar toxic effect of 100% extract of pure Zn has also been reported on MG-63 cells [137,138]. Genotoxicity refers to the damage on genetic materials such as DNA damage, gene mutation and impaired DNA repairment [139]. Murni et al. [140] claimed that the pure Zn extract will cause mild necrosis and significant DNA damage of NHOst cells. Alloying with other elements can alter the physiological response of Zn efficiently. Plenty of researches have reported that the addition of Mg can improve the biocompatibility of Zn. Murni et al. [140] pointed out that alloying with Mg can significantly alleviate the genotoxicity of Zn in Zn–3Mg alloy. In addition, Kubásek et al. [141] also confirmed that there was no significant DNA damage of U-2 OS cell line when cultured in the extract of Zn-0.8 Mg alloy. Similar positive influence of the addition of Mg on cell proliferation has also been reported on Zn-0.05 Mg [107] and Zn-0.5Al-xMg (x = 0.1, 0.3 and 0.5) alloys [142]. Besides, during the degradation of Zn–Mg alloy, the bone-like components such as skorpionite and hydroxyapatite are supposed to stimulate the osseointegration [143]. In addition, the beneficial effects of Ca and Sr as alloying elements on cytocompatibility have also been proved [132].

So far, the *in vivo* biocompatibility studies of Zn-based BMs for orthopedic applications are relatively limited, as summarized in Fig. 5 and Table 2. It is revealed that excessive release of Zn ions resulted in the poor osseointegration *in vivo* (Figure 5a and 5d-f). Yang et al. [146] implanted the pure Zn into the rat femur condyle. A serious fibrous tissue encapsulation was found for pure Zn, resulting in the lack of direct bonding between bone and implant (Fig. 5e). The delayed osseointegration of pure Zn is claimed to be attributed to the local high Zn ion concentration. In consistence with the observations *in vitro*, the *in vivo* results confirmed that alloying with appropriate elements such as Mg, Ca and Sr can effectively improve the biocompatibility (Fig. 5a). Li et al. [132] indicated that Zn–1Mg, Zn–1Ca and Zn–1Sr alloys were able to improve the new bone formation after two months of implantation (Fig. 5b). Meanwhile, compared with Mg, the promoting effects of Ca and Sr were superior with a ranking of Zn–1Sr > Zn–1Ca > Zn–1Mg. A favorable *in vivo* osteogenesis was found around Zn-0.05 Mg alloy as well (Fig. 5c) [107]. As for the ternary alloys, the addition of any two of these elements also confirmed better cytocompatibility with Zn–1Ca–1Sr ranking the best, which is in agreement with the finding in binary alloys [152]. In addition, the fabrication of metal matrix composite is another efficient way to improve the biocompatibility of Zn. Yang et al. [146] fabricated Zn-hydroxyapatite biocomposite by spark plasma sintering and achieved an increased corrosion rate with better cytocompatibility. However, although superior new bone formation was found compared with pure Zn, the lack of direct bone bonding of Zn-hydroxyapatite biocomposite *in vivo* suggested delayed osseointegration (Fig. 5f). In addition, the incorporation of Mg into Zn by spark plasma sintering exhibited accelerated corrosion behavior and better osteointegration with sacrificial Mg-rich anode as shown in Fig. 5g [145].

Biocompatibility is the ability of a material to perform its desired functions in accordance to a medical therapy with the most appropriate host response in that specific situation, instead of causing any adverse local or systemic effects [158]. In comparison with Fe and Mg, the tolerance value of organism to Zn is much lower. It is noted that the recommended daily intake (RDI) value for Zn (6.5–15 mg) is similar to that of Fe (10–20 mg), but much lower than that of Mg (375–700 mg)

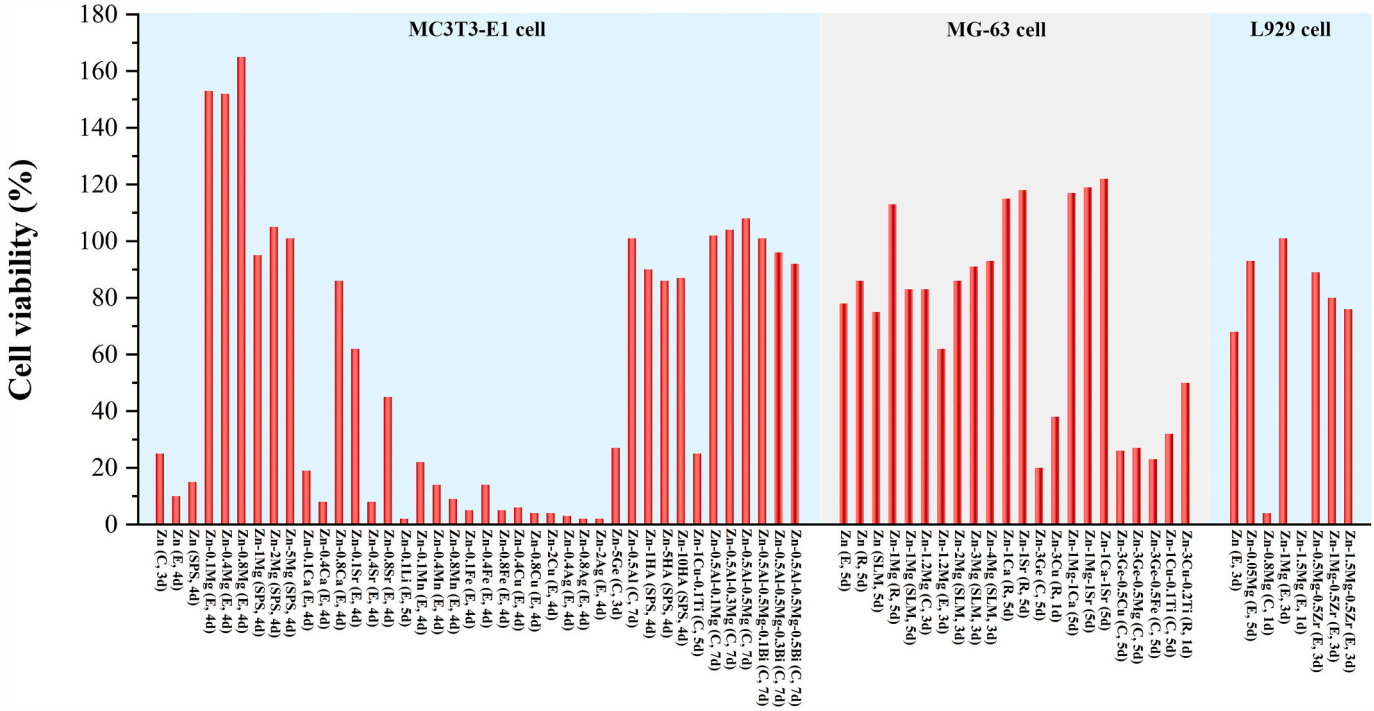

Fig. 4. Summary of reported cell viabilities of MC3T3-E1 cells, MG-63 cells and L929 cells cultured in the 100% extracts of Zn-based BMs for orthopedic applications (The annotation in the bracket shows the working history of the materials and the culturing time of cells. C, E, R, SPS and SLM refer to cast, extruded, rolled, spark plasma sintering and selective laser melting, respectively.) [107,109,132,135,137,138,141,142,144–155].

[95]. In addition, the serum concentration of Zn is 0.012–0.018 mmol L^{-1}, which is similar to that of Fe (0.013–0.031 mmol L^{-1}), but much lower than that of Mg (0.7–1.0 mmol L^{-1}) [108]. *In vitro* cytocompatibility assay also demonstrated that the viabilities of MC3T3-E1 and L929 cells were more sensitive to the concentration of Zn ions in contrast with that of Mg and Fe ions. Yamamoto et al. [159] studied the cytotoxicity of 43 metal salts to murine fibroblasts and osteoblastic cells. The IC_{50} values of MC3T3-E1 cell and L929 cell for Fe^{3+} (3.28×10^{-4} mol L^{-1} and 5.42×10^{-3} mol L^{-1}) are much higher than those of Zn^{2+} (9×10^{-5} mol L^{-1} and 9.28×10^{-5} mol L^{-1}), demonstrating a better cytocompatibility of Fe^{3+}. Note that the IC_{50} value of Mg^{2+} is seldom studied, Mg salt is indispensably required to be provided for cell culture. The amount of Mg^{2+} in DMEM is approximately 8.13×10^{-4} mol L^{-1}, which is obviously higher than the IC_{50} values of Zn^{2+} [160]. The median lethal dose (LD_{50}) is generally utilized to evaluate the *in vivo* biocompatibility and long-term chronic toxicity of metallic elements. The LD_{50} values of the chloride of element Zn is 350 mg kg^{-1}, far below the values of the chloride of Fe (1300 mg kg^{-1}) and Mg (5000 mg kg^{-1}) [108]. Hence, although Zn-based BMs stand out with superior corrosion behavior, more attention should be focused on their biosafety in consideration of the threshold concentration to cause biotoxicity.

2.3. *In vitro and in vivo degradation behavior and biocompatibility studies on Zn-based BMs for cardiovascular applications*

In comparison with the traditional permanent metallic stents, biodegradable metallic stents are bioactive and only provide provisional support until vessel healing. Therefore, some long-term clinical issues corresponding to the persistent existence of stents, including the chronic inflammation, stent thrombosis, in-stent restenosis and prolonged antiplatelet therapy, can be avoided [161,162]. The first attempt of application of Zn-based BMs in cardiovascular environment can be traced to 2013. Bowen et al. [111] implanted pure Zn wires into the abdominal aorta of adult male Sprague-Dawley rats up to six months. It was claimed pure Zn can maintain mechanical stability during the initial four months and, subsequently, it showed accelerated disintegration, demonstrating the near-ideal biocorrosion behavior for cardiovascular stent applications. From then on, numerous researches have been focused on the development of Zn-based BMs for cardiovascular applications. There are 51 publications regarding Zn-based BMs for cardiovascular applications since 2017 when analyzed via Web of Science database with the topics of Zn alloy and stent. Nonetheless, the mechanical properties of pure Zn are not strong enough for cardiovascular stent, hampering its further applications. The tensile strength and elongation of as-cast pure Zn are only 20 MPa and 0.3%, far below the clinical requirements as shown in Table 1 [163]. Therefore, diverse improvement methods including alloying and thermomechanical treatments have been adopted to realize the applications of Zn-based BMs in cardiovascular field. As summarized in Table 3, tailoring the composition and microstructure will lead to changes in the mechanical properties, corrosion behavior and biocompatibility of Zn-based BMs. Alloying with metallic elements such as Li, Mg, Ca, Sr, Mn, Cu and Ag can significantly improve the mechanical performance of Zn-based BMs.

The reported *in vivo* researches of Zn-based BMs for cardiovascular applications are displayed in Fig. 6 and Table 4. Yang et al. [164] implanted pure Zn stents into the abdominal aortas of adult Japanese rabbits (Fig. 6a). It was found that there was no phenomenon of severe inflammatory response, platelet aggregation, thrombosis formation and intimal hyperplasia after the implement of pure Zn stents. The mechanical integrity of stents maintained stable for 6 months, while the stent volume decreased by 41.75 ± 29.72% after 12 months' implantation. Zhou et al. [165] implanted Zn-0.8Cu alloy stents into the porcine coronary arteries for 24 months and demonstrated the absence of inflammation and thrombosis formation (Fig. 6b). Later on, Zn–3Ag alloy stents were fabricated and implanted into the iliofemoral arteries of juvenile domestic pigs by Hehrlein et al. [166]. Excellent vascular healing was observed with no signs of thrombosis or vascular occlusion (Fig. 6c). Jin et al. [167] implanted Zn-xMg (x = 0.002, 0.005 and 0.08) alloy wires into the abdominal aorta of adult male Sprague-Dawley rats (Fig. 6d). It was claimed that a mild inflammation and intimal activation

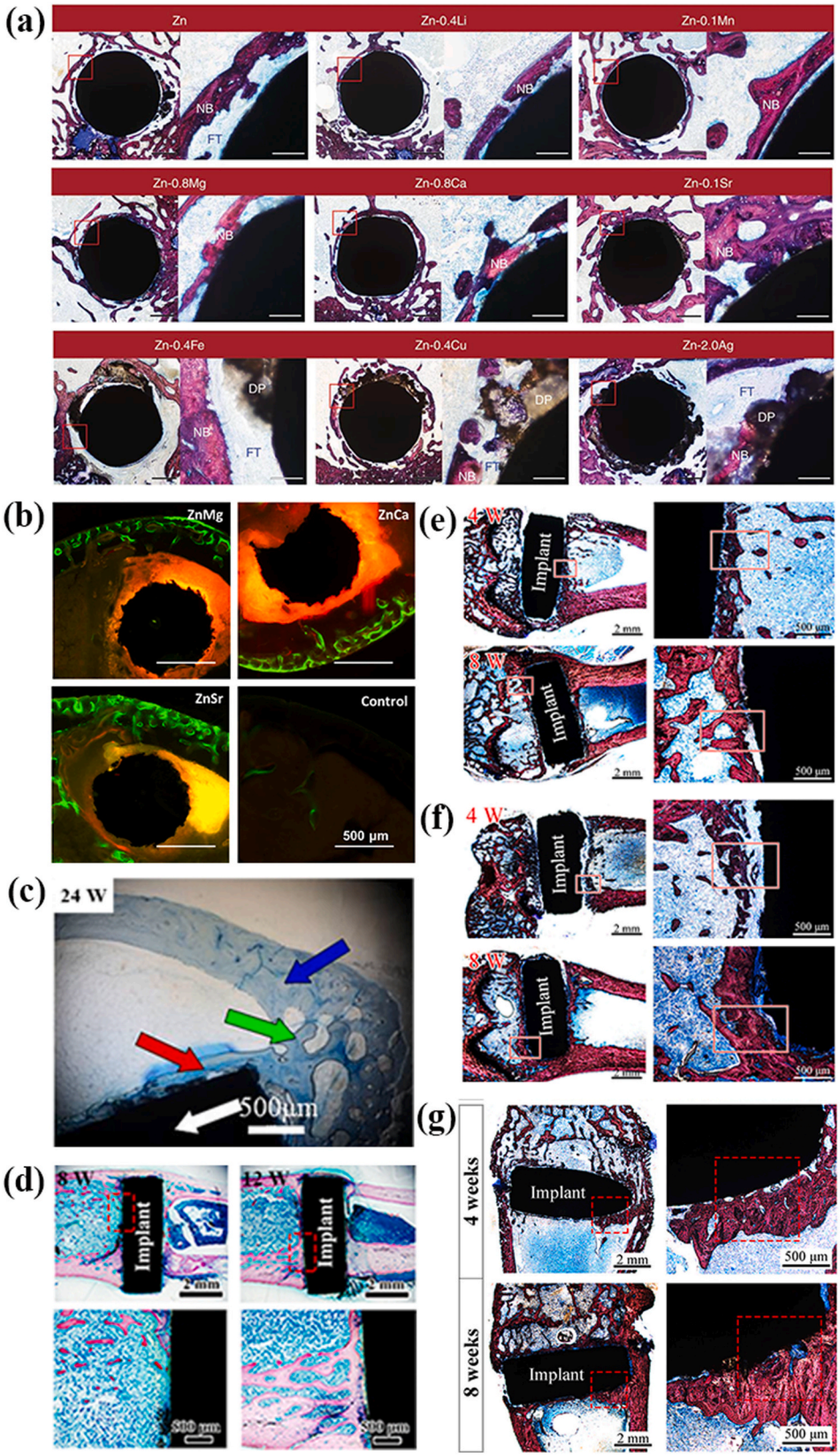

Fig. 5. Representative *in vivo* biocompatibility of Zn-based bone implants in the literature: (a) Hard tissue sections of pure Zn, Zn-0.4Li, Zn-0.1Mn, Zn-0.8 Mg, Zn-0.8Ca, Zn-0.1Sr, Zn-0.4Fe, Zn-0.4Cu and Zn–2Ag in metaphysis. The magnified region is marked by red rectangle. NB, new bone; DP, degradation products; FT, fibrous tissue. Scale bar, 0.5 mm in low magnification, 500 μm in high magnification. (Reproduced with permissions from Ref. [109]). (b) Histological sections of mouse distal femoral shaft from Zn–1Mg, Zn–1Ca, Zn–1Sr implanted pins groups and the sham control group observed under fluorescent microscopy at week 8. (Reproduced with permissions from Ref. [132]). (c) Histological section of Zn-0.05 Mg implanted in rabbit tibial shaft for 24 weeks. There are normal cortical bones (blue arrow); implant (white arrow); newly formed bone fractions around the implant (red arrow); bone junction between cortical bone and new bone formation (green arrow). (Reproduced with permissions from Ref. [107]). (d) Hard tissue sections of the Zn-0.1Li alloy after 8 and 12 weeks' implantation in rat femur condyle. (Reproduced with permissions from Ref. [135]). Hard tissue sections of (e) pure Zn (Reproduced with permissions from Ref. [146]), (f) Zn-5HA composite (Reproduced with permissions from Ref. [146]) and (g) Zn–5Mg composite (Reproduced with permissions from Ref. [145]) fabricated by spark plasma sintering after being implanted in the rat femur condyle for 4 and 8 weeks. The red rectangles correspond to the magnified bone-implant interface. The red triangle indicates newly formed bone. (For interpretation of the references to colour in this figure legend, the reader is referred to the Web version of this article.)

can be observed. Besides, it seems that the biocompatibility became worse with the increase in Mg content, which might be attributed to the formation of intermetallics. Zhao et al. [168] implanted Zn-0.1Li alloy wires into the abdominal aorta of rats and found that Zn-0.1Li alloy system exhibited a moderate inflammatory response without obstructive neointima (Fig. 6e). Zn-xAl (x = 1, 3 and 5) alloy stripes were implanted into the wall of the abdominal aorta of adult Sprague-Dawley rats by Bowen et al. [169]. It was demonstrated that a moderate inflammatory

Table 2
Summary of the *in vivo* biocorrosion and biocompatibility properties of biodegradable Zn-based BMs for orthopedic applications.

Material	Working history	Animal mode	Implantation site	Period time	Corrosion rates (μm/year)	Inflammatory reactions	Capsule formation	New bone formation	Bone contact	Ref.
Pure Zn	Extruded	Sprague Dawley rat	Medullary cavity of femoral shaft	8 w	~140	NA	+	+	+	[109]
Pure Zn (99.95%)	Extruded	New Zealand rabbit	Tibial shaft	24 w	NA	–	+	+	–	[107]
Pure Zn (99.998%)		Sprague Dawley rat	Calvaria	10 w	~44	NA	+	+	NA	[156]
Pure Zn	Spark plasma sintering	Sprague Dawley rat	Femoral condyle	8 w	NA	+	+	+	–	[146]
Zn–1Mg	Rolled	C57BL/6 mice	Medullary cavity of femoral shaft	8 w	170	–	NA	+	NA	[132]
Zn–1Ca	Rolled	C57BL/6 mice	Medullary cavity of femoral shaft	8 w	190	–	NA	+	NA	[132]
Zn–1Sr	Rolled	C57BL/6 mice	Medullary cavity of femoral shaft	8 w	220	–	NA	+	NA	[132]
Zn-0.1Li	Extruded	Sprague-Dawley rat	Femur condyle	12 w	NA	+	+	+	+	[135]
Zn-0.1Mn	Extruded	Sprague Dawley rat	Medullary cavity of femoral shaft	8 w	~130	NA	+	+	+	[109]
Zn-0.8Ca	Extruded	Sprague Dawley rat	Medullary cavity of femoral shaft	8 w	~130	NA	+	+	+	[109]
Zn-0.05Mg	Extruded	New Zealand rabbit	Tibial shaft	24 w	NA	–	+	+	+	[107]
Zn-0.8Mg	Extruded	Sprague Dawley rat	Medullary cavity of femoral shaft	8 w	~140	NA	+	+	+	[109]
Zn–5Mg	Spark plasma sintering	Sprague Dawley rat	Femoral condyle	8 w	NA	–	+	+	+	[145]
Zn-0.1Sr	Extruded	Sprague Dawley rat	Medullary cavity of femoral shaft	8 w	~150	NA	+	+	+	[109]
Zn-0.4Fe	Extruded	Sprague Dawley rat	Medullary cavity of femoral shaft	8 w	~150	NA	+	+	+	[109]
Zn-0.4Li	Extruded	Sprague Dawley rat	Medullary cavity of femoral shaft	8 w	~170	NA	+	+	+	[109]
Zn-2.0Ag	Extruded	Sprague Dawley rat	Medullary cavity of femoral shaft	8 w	~180	NA	+	+	+	[109]
Zn-0.4Cu	Extruded	Sprague Dawley rat	Medullary cavity of femoral shaft	8 w	~260	NA	+	+	+	[109]
Zn-0.8Mn	Extruded	Rat	Femoral condyle	12 w	NA	NA	NA	+	NA	[157]
Zn-5HA	Spark plasma sintering	Sprague Dawley rat	Femoral condyle	8 w	NA	+	+	+	–	[146]

Note: +: Positive; -: Negative; NA: Not available.

response without any signs of necrosis took place after implantation (Fig. 6f).

3. Surface modification of Zn-based BMs for biomedical applications

3.1. Surface modification of Zn-based BMs for orthopedic applications

The interactions between the tissues and implants are directly associated with the surface characteristics of the implants. Surface modification is one of the most efficient way to improve the surface properties of implanted materials and endow them with new functions. In comparison with alloying or compositing, surface modification only alters the surface characteristics of Zn-based BMs, maintaining the original performance of bulk materials. So far, the primary aim of the limited reports on the surface modification of biodegradable Zn-based BMs for orthopedic applications is to construct a temporary surface featured by the proper corrosion behavior and superior biocompatibility. The development and representative surface morphologies of Zn-based BMs after different surface modifications for orthopedic applications are summarized in Table 5 and Fig. 7.

(1) Phosphate conversion coating

Zinc phosphate has been put forward as versatile material for biomedical applications [195,196]. It can stimulate the adsorption of Ca^{2+} ascribed to the existence of PO_4^{3-}. Meanwhile, it is also reported that zinc phosphate has a stimulative effect on the growth of hydroxyapatite under the condition of immersion in simulated body fluid [197]. Su et al. [136] investigated the zinc phosphate coating fabricated by immersing pure Zn discs in the mixed solution of $Zn(NO_3)_2$ and H_3PO_4. They found that the zinc phosphate coating improved the cell viability, adhesion and proliferation of pre-osteoblasts while suppressed the adhesion of *E. coli*, which is attributed to the decreased Zn ions release and micro/nano surface topography.

(2) Biomimetic deposition

Generally, biomimetic process proceeds when the samples are immersed in aqueous solutions of supersaturated calcium and phosphate, resulting in the formation of calcium phosphate coating on the surface [198]. Jablonská et al. [155] pretreated the Zn-1.5 Mg alloy in the simulated body fluid at 37 °C for 14 days. Consequently, a layer of protective film, abundant in calcium phosphate, was generated on the surface. The resulting coating led to improved corrosion resistance as well as better cell viability and adhesion of U-2 OS cells.

(3) Organic and polymer coating

The biodegradable organic and polymer coatings can protect the

Table 3
Summary of the mechanical properties, *in vitro* biodegradability and biocompatibility of the reported Zn-based BMs for cardiovascular applications.

Material	Working history	Mechanical properties			*In vitro* corrosion			*In vitro* cytocompatibility		Ref.
		Ultimate tensile strength (MPa)	Tensile yield strength (MPa)	Elongation (%)	Corrosion medium	Electrochemical test (mm/year)	Immersion test (mm/year)	Cell line	Cell viability	
Zn (99.99%)	Cast	18.25 ± 2.99	10.14 ± 2.32	0.32 ± 0.08						[132]
Zn (99.99%)	Rolled	~48.7	~30.0	~5.6	Hank's solution	~0.13	~0.08	Human umbilical vein endothelial cell (ECV304) Rodent vascular smooth muscle cell (VSMC)	~88% (5d, 100% extract) ~72% (5d, 100% extract)	[132]
Zn (99.99%)	Extruded	~63.7	~34.2	~3.5						[132]
Zn (99.995%)	Extruded	111 ± 4.5	51 ± 3.7	60 ± 5.9	Hank's modified solution	~0.13	~0.07			[170]
Zn (99.99+%)					Hank's solution	0.56 ± 0.18		Human endothelial cell (EA.hy926) Human aortic vascular smooth cell (HA-VSMC)	~20% (5d, 100% extract) ~30% (5d, 100% extract)	[171]
Zn	Rolled	~142	~111	36 ± 2						[169]
Zn	Selective laser melting	~132	~108	~12						[172]
Zn-0.002Mg	Extruded	63 ± 9	34 ± 4	17 ± 3						[167]
Zn-0.005Mg	Extruded	202 ± 60	93 ± 1	28 ± 2						[167]
Zn-0.08Mg	Extruded	339 ± 42	221 ± 14	40 ± 3						[167]
Zn-0.15Mg	Extruded	250 ± 9.2	114 ± 7.7	22 ± 4.0	Hank's modified solution	~0.16	~0.08			[170]
Zn-0.02Mg	Extruded	231.51 ± 3.56	188.67 ± 6.19	31.08 ± 3.41	Hank's solution	0.093 ± 0.006		Human umbilical vein endothelial cell (HUVEC)	~108 (3d, 100% extract)	[173]
Zn-0.05Mg	Rolled	227 ± 5	197 ± 4	34 ± 3						[174]
Zn-0.5Mg	Extruded	297 ± 6.5	159 ± 8.5	13 ± 0.9	Hank's modified solution	~0.16	~0.08			[170]
Zn–1Mg	Cast	184.84 ± 20.91	127.98 ± 10.72	1.82 ± 0.23						[132]
Zn–1Mg	Rolled	~235.5	~187.9	11.8	Hank's solution	~0.15	~0.08	Human umbilical vein endothelial cell (ECV304) Rodent vascular smooth muscle cell (VSMC)	~101% (5d, 100% extract) ~70% (5d, 100% extract)	[132]
Zn–1Mg	Extruded	~266.3	~205.4	8.4						[132]
Zn–1Mg	Extruded	340 ± 15.6	180 ± 7.3	6 ± 1.1	Hank's modified solution	~0.17	~0.08			[170]
Zn–3Mg	Extruded	399 ± 14.4	291 ± 9.3	1 ± 0.1	Hank's modified solution	~0.13	~0.08			[170]
Zn–1Ca	Cast	164.57 ± 13.92	119.12 ± 7.01	2.10 ± 0.23						[132]
Zn-1Ca	Rolled	~251.8	~204.9	~12.6	Hank's solution	~0.16	~0.09	Human umbilical vein endothelial cell (ECV304) Rodent vascular smooth muscle cell (VSMC)	~100% (5d, 100% extract) ~70% (5d, 100% extract)	[132]
Zn-1Ca	Extruded	~242.4	~201.5	~7.6						[132]
Zn–1Sr	Cast	171.40 ± 14.13	120.21 ± 6.08	2.03 ± 0.22						[132]
Zn–1Sr	Rolled	~227	~187.4	~19.7	Hank's solution	~0.17	~0.10	Human endothelial cell (ECV304) Rodent vascular smooth muscle cell (VSMC)	~102% (5d, 100% extract) ~73% (5d, 100% extract)	[132]
Zn-1Sr	Extruded	~265.3	~217.4	~10.6						[132]
Zn-0.1Li	Extruded	274 ± 61	238 ± 60	17 ± 7						[168]
Zn-0.5Li	Extruded	364.9	22							[175]

(*continued on next page*)

Table 3 (*continued*)

Material	Working history	Mechanical properties			*In vitro* corrosion			*In vitro* cytocompatibility		Ref.
		Ultimate tensile strength (MPa)	Tensile yield strength (MPa)	Elongation (%)	Corrosion medium	Electrochemical test (mm/year)	Immersion test (mm/year)	Cell line	Cell viability	
Zn–2Li	Rolled	~364	~238	~14.3	Modified SBF solution	0.06				[176]
Zn–4Li	Rolled	~440	~423	~13.7	Modified SBF solution	0.05				[176]
Zn–6Li	Rolled	~562	~473	~2.3	Modified SBF solution					[176]
Zn–1Cu	Extruded	186.3 ± 0.5	148.7 ± 0.5	21.0 ± 4.4	c-SBF solution		~0.033	Human endothelium-derived cell (EA.hy926)	~37% (5d, 100% extract)	[177]
Zn–2Cu	Extruded	240.0 ± 1.4	199.7 ± 4.2	46.8 ± 1.4	c-SBF solution		~0.027	Human endotheium-derived cell (EA.hy926)	~11% (5d, 100% extract)	[177]
Zn–3Cu	Extruded	257.0 ± 0.81	213.7 ± 1.2	47.2 ± 1.0	c-SBF solution		~0.030	Human endothelium-derived cell (EA.hy926)	~60% (5d, 100% extract)	[177]
Zn–3Cu	Extruded	288 ± 4.03	~288	45.9 ± 3.33	SBF solution	0.0852	0.0453 ± 0.00822	Human umbilical vein endothelial cell (EA.hy926)	~64%(3d, 100% extract)	[178, 179]
								Rat thoracic aorta smooth muscle cell (A7r5)	~48% (3d, 100% extract)	
Zn–4Cu	Extruded	270 ± 10	250 ± 10	51 ± 2	Hank's solution		0.00941 ± 0.00134	Human endothelial cell (EA.hy926)	~20% (5d, 100% extract)	[180]
Zn-0.2Mn	Extruded	220	132	48						[181]
Zn-0.6Mn	Extruded	182	118	91						[181]
Zn-2.5Ag	Extruded	~203	~147	35	Hank's modified solution	0.137 ± 0.021	0.079 ± 0.007			[182]
Zn–3Ag	Extruded	240–260	130–145	70–135						[166]
Zn-5.0 Ag	Extruded	~253	~208	37	Hank's modified solution	0.144 ± 0.007	0.081 ± 0.001			[182]
Zn-7.0Ag	Extruded	~287	~236	32	Hank's modified solution	0.147 ± 0.018	0.084 ± 0.005			[182]
Zn-0.5Al	Extruded	203 ± 9.6	119 ± 2.3	33 ± 1.2	Hank's modified solution	~0.14	~0.08			[170]
Zn–1Al	Extruded	223 ± 4.3	134 ± 5.8	24 ± 4.2	Hank's modified solution	~0.14	~0.08			[170]
Zn–1Al	Rolled	~238	~197	~24						[169]
Zn–3Al	Rolled	~224	~203	~31						[169]
Zn–5Al	Rolled	~308	~240	~16						[169]
Zn-0.02Mg-0.02Cu	Extruded	262.25 ± 5.02	216.2 9 ± 3.27	27.74 ± 2.21				Human umbilical vein endothelial cell (HUVEC)	~99% (3d, 100% extract)	[183]
Zn-0.02Mg-0.02Cu	Extruded	262.25 ± 5.02	216.29 ± 3.27	27.74 ± 2.21	Hank's solution	0.079 ± 0.004	0.047 ± 0.005			[184]
Zn–3Cu-0.5Fe	Extruded	284 ± 1.63	~231	32.7 ± 4.17	SBF solution	0.1045	0.0643 ± 0.00403	Human umbilical vein endothelial cell (EA.hy926)	~54% (3d, 100% extract)	[178, 179]
								Rat thoracic aorta smooth muscle cell (A7r5)	~31% (3d, 100% extract)	
Zn–3Cu–1Fe	Extruded	272 ± 7.48	~219	19.6 ± 1.36	SBF solution	0.1301	0.0689 ± 0.00734	Human umbilical vein endothelial cell (EA.hy926)	~47% (3d, 100% extract)	[178, 179]
								Rat thoracic aorta smooth muscle cell (A7r5)	~21% (3d, 100% extract)	
Zn-1.5Cu-1.5Ag	Cast	77.2 ± 2.25	75.3 ± 2.49	0.54 ± 0.09						[185]
Zn-1.5Cu-1.5Ag	Extruded	220.3 ± 1.70	162.0 ± 2.94	44.13 ± 1.09	c-SBF solution	0.019 ± 0.00086	0.0486 ± 0.00414	Human umbilical vein endothelial cell (EA.hy926)	~19% (3d, 50% extract)	[185]
	Extruded	~366	~345	~5.3		0.01757	~0.022			[186]

(*continued on next page*)

Table 3 (*continued*)

Material	Working history	Mechanical properties			*In vitro* corrosion			*In vitro* cytocompatibility		Ref.
		Ultimate tensile strength (MPa)	Tensile yield strength (MPa)	Elongation (%)	Corrosion medium	Electrochemical test (mm/year)	Immersion test (mm/year)	Cell line	Cell viability	
Zn–3Cu-0.1Mg					Hank's solution			Human endothelium-derived cell (EA.hy926)	~74% (5d, 100% extract)	
Zn–3Cu-0.5Mg	Extruded	~418	~404	~2.1	Hank's solution	0.02362	~0.030	Human endothelium-derived cell (EA.hy926)	~88% (5d, 100% extract)	[186]
Zn–3Cu-1.0Mg	Extruded	~441	~428	~1.0	Hank's solution	0.18048	~0.043	Human endothelium-derived cell (EA.hy926)	~92% (5d, 100% extract)	[186]
Zn-0.1Mn-0.05Mg	Rolled/naturally aged	274 ± 5	230 ± 3	41 ± 1						[174]
Zn-0.5Cu-0.05Mg	Rolled/naturally aged	312 ± 2	241 ± 5	44 ± 2						[174]
Zn-0.75Mn-0.40Cu	Cast	120.1 ± 3.2	113.2 ± 0.2	0.4 ± 0.1						[187]
Zn-0.75Mn-0.40Cu	Rolled	277.5 ± 3.7	195.5 ± 10.7	15.3 ± 3.9	SBF solution	0.062 ± 0.009	0.050 ± 0.004			[187]
Zn-0.35Mn-0.41Cu	Cast	83.9 ± 0.4	76.7 ± 0.3	0.3 ± 0.1						[187]
Zn-0.35Mn-0.41Cu	Rolled	292.4 ± 3.4	198.4 ± 6.7	29.6 ± 3.8	SBF solution	0.098 ± 0.005	0.065 ± 0.006			[187]

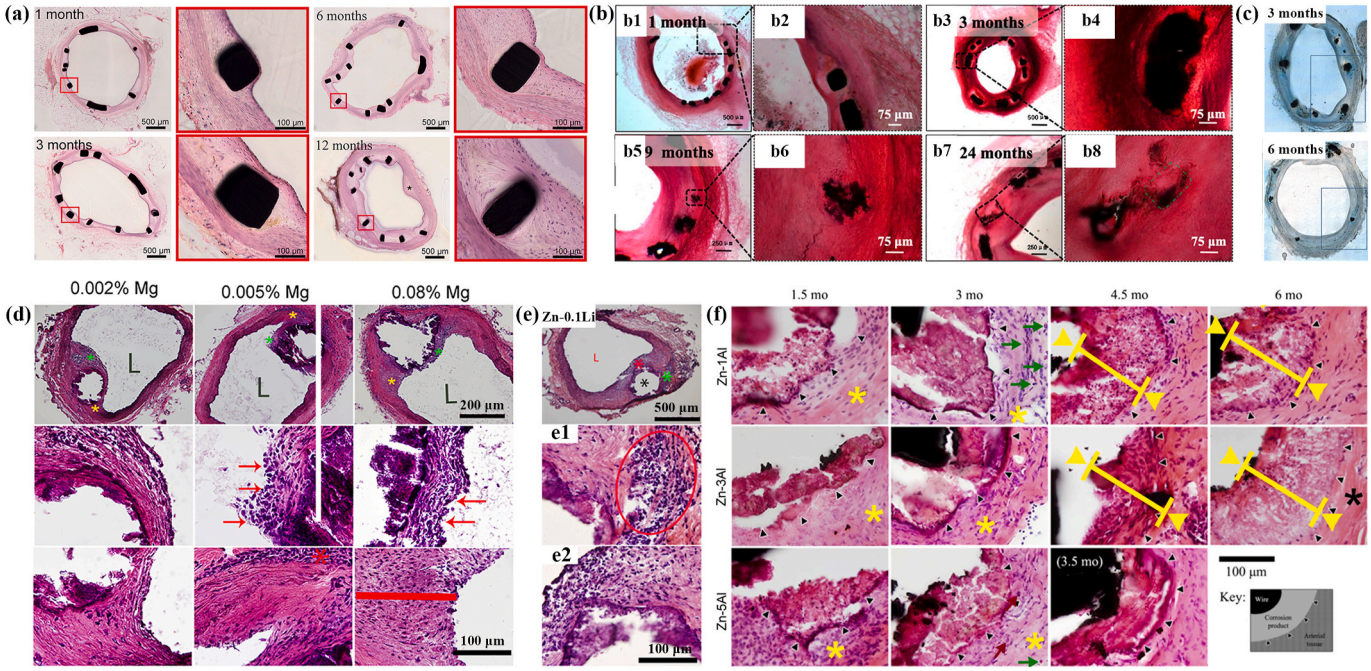

Fig. 6. Representative *in vivo* biocompatibility of Zn-based cardiovascular implants in the literature: (a) hematoxylin-eosin (H&E) stained sections of abdominal aorta after 1, 3, 6 and 12 months' implantation of pure Zn stents. (Reproduced with permissions from Ref. [164]). (b) H&E-stained cross-sections after implantation of Zn-0.8Cu alloy stents in the porcine coronary arteries for 1, 3, 9, 24 months. (Reproduced with permissions from Ref. [165]). (c) Histologic images of representative cross-sections of porcine iliofemoral arteries stented with a Zn–3Ag bioresorbable vascular stent after 3 and 6 months. (Reproduced with permissions from Ref. [166]). (d) H&E staining of 6-months implanted Zn-0.002 Mg, Zn-0.005 Mg, and Zn-0.08 Mg alloy wires through the arterial lumen at different magnifications. 2nd and 3rd rows correspond to green and yellow asterisks respectively at high magnifications. L denotes the luminal opening. (Reproduced with permissions from Ref. [167]). (e) H&E staining of Zn-0.1Li alloy wires after 11months' implantation in the abdominal aorta of Sprague Dawley rat. Low magnification images show two subsequent areas selected for high magnification. "L" is the luminal opening of the artery. (Reproduced with permissions from Ref. [168]). (f) H&E staining of Zn–xAl alloy (x = 1, 3 and 5) strips after implantation in the wall of the abdominal aorta of adult Sprague-Dawley rats for 1.5–6 months. Black triangles mark the interface between the native adventitial tissue and corroding product/remodeled tissue. (Reproduced with permissions from Ref. [169]). (For interpretation of the references to colour in this figure legend, the reader is referred to the Web version of this article.)

Table 4
Summary of the *in vivo* biocorrosion and biocompatibility properties of biodegradable Zn-based BMs for cardiovascular applications.

Material	Implant shape	Animal mode	Implantation site	Period time	*In vivo* corrosion rate (mm/year)	Inflammatory response	Thrombosis	Intimal hyperplasia	Ref.
Pure Zn (99.995%)	Stent	Adult Japanese rabbit	Abdominal aorta	12 months	NA	–	–	–	[164]
Pure Zn	Wire	Rat	Abdominal aorta	11 months	NA	NA	NA	-	[188]
Pure Zn (99.99+%)	Wire	Male young CD IGS rat	Abdominal aorta	6 months	NA	+	NA	NA	[171]
Pure Zn (99.99+%)	Wire	Sprague Dawley rat	Abdominal aorta	6.5 months	NA	-	-	-	[189]
Zn-0.002Mg	Wire	Adult male Sprague-Dawley rat	Abdominal aorta	11 months	~0.027 at 4.5 months and ~0.050 at 11 months	+	NA	+	[167]
Zn-0.005Mg	Wire	Adult male Sprague-Dawley rat	Abdominal aorta	11 months	~0.023 at 4.5 months and ~0.039 at 11 months	+	NA	+	[167]
Zn-0.08Mg	Wire	Adult male Sprague-Dawley rat	Abdominal aorta	11 months	~0.015 at 4.5 months and ~0.023 at 11 months	+	NA	+	[167]
Zn-0.8Cu	Stent	Female Shanghai white pig	Left anterior descending artery, left circumflex artery, or right coronary artery	24 months	~0.016 at 3 months	+	–	+	[165]
Zn–3Ag	Stent	Juvenile domestic swine	Iliofemoral artery	6 months	NA	NA	–	NA	[166]
Zn-0.1Li	Wire	Sprague Dawley rat	Abdominal aorta	12 months	~0.019 at 9 months and ~0.046 at 12 months	+	NA	+	[168]
Zn–4Li	Wire	Rat	Abdominal aorta	11 months	NA	NA	NA	+	[188]
Zn-0.02Mg-0.02Cu	Stent	New Zealand white rabbit	Left carotid artery	12 months	~0.025 at 3–6 months and 0.040 ± 0.013 at 12 months	NA	NA	+	[183]

Note: +: Positive; -: Negative; NA: Not available.

substrate from the attack of aggressive corrosion media in physiological environment, which has been widely applied in the corrosion protection of BMs [199–201]. Besides, the ability of drug delivery and functioning with other biomolecules also render them promising alternatives. Collagen coating has been proposed to modify the surface of pure Zn via dip-coating by Su et al. [136]. The collagen coating exhibited a favorable impact on the corrosion resistance and cytocompatibility for pre-osteoblasts and endothelial cells.

(4) Electrochemical method

Anodic oxidation (ANO) involves a process of electrolytic passivation which can grow a stable and uniform oxide film with controllable and desired thickness on the anode surface. It is reported that various nanostructures can be constructed on the surface of Zn after anodic oxidation including nanowires [202], nanostrips [203], nanosheets [204], nanotubes [205] and so on. Gilani et al. [206] constructed ZnO micro/nano hole array and nanopariticle array on Zn foil by anodic oxidation and demonstrated superior antibacterial property against both Gram-negative *E. coli* and Gram-positive *S. aureus*. Besides, Lyu et al. [207] fabricated dexamethasone-laden ZnO nanotube on Zn substrate by anodic oxidation followed by silk fibroin/graphene self-assembly. They found that this composite coating enhanced the biocompatibility and antibacterial property due to the synergistic release of Zn ions and drug during degradation.

In contrast with anodic oxidation, microarc oxidation (MAO) treatment proceed under a high-voltage discharge. Homogeneously distributed micropores are formed on the surface during the microarc oxidation process when the molten oxide and gas bubble are ejected through the microarc discharge channel. MAO technology has been widely applied to construct porous, rough and adherent oxide coating on the surface of metals such as magnesium [208,209], aluminum [210, 211] and titanium [212]. Meanwhile, calcium, phosphorus or other elements can be incorporated into the oxide layer by adding corresponding electrolyte ingredients, improving the osteogenesis and biocompatibility [213]. Yuan et al. [137] fabricated microarc oxidation coating incorporated with CaP compound on the surface of pure Zn. Instead of improved corrosion resistance that have been found on Mg alloys, they found that MAO coating accelerated the corrosion rate of pure Zn due to anabatic chemical dissolution and galvanic corrosion between the coating and substrate.

(5) Atomic layer deposition

Atomic layer deposition (ALD) has been put forward as a promising approach of depositing nanofilm in a variety of applications. ALD shows advantages of precise control over material thickness and composition at angstrom level [214]. In addition, a layer of extremely smooth and conformal film can be generated on both flat surface and high aspect ratio structures after ALD treatment [215]. In terms of biomedical applications, different metallic oxide films have been constructed on the surface of Mg-based BMs via ALD as coating materials to improve their corrosion resistance and biocompatibility [216]. Recently, Yuan et al. [135] prepared a layer of homogeneous ZrO_2 film with the film thickness ranging from 40 nm to 120 nm on the surface of Zn–Li alloy by means of ALD. They found a beneficial effect of the ZrO_2 nanofilm on the corrosion resistance of Zn–Li alloy, accompanied by a less release of Zn^{2+} in corrosion media. Meanwhile, better *in vitro* cell adhesion and proliferation as well as *in vivo* osseointegration were demonstrated after ALD treatment.

(6) Magnetron sputtering

Magnetron sputtering has been widely applied to deposit high-quality functional coatings on the surface of diverse materials [217, 218]. Peng et al. [193] produced diamond-like carbon (DLC) film on the

Table 5
Summary of different surface modification methods of Zn-based BMs for orthopedic applications.

Surface modification method		Substrate	Techniques and modified layer	Main layer structure	Layer thickness	*In vitro* corrosion rate (mm/y)			*In vitro* biocompatibility			*In vivo* Biocompatibility	Ref.
						Corrosion medium	Electrochemical test	Immersion test	Cell line	Cytocompatibility	Hemocompatibility		
chemical method	Phosphate conversion coating	Pure Zn (99.99+%)	Immersing in 0.07 M $Zn(NO_3)_2$ and 0.15 M H_3PO_4 solution, pH 2-3	Zinc phosphate	5–6 μm	Hank's solution	0.004 ± 0.001		i. Murine calvarial pre-osteoblast (MC3T3-E1) ii. Human endothelial cell (EA. hy926)	Improved cell adhesion, proliferation and differentiation Improved cell adhesion and proliferation	Both platelets adhesion and hemolysis tests showed good hemocompatibility with no sign of thrombogenicity		[136]
		Pure Zn (99.99%)	Immersion in the mix solution of 0.07 M Zn $(NO_3)_2$, 0.15 M H_3PO_4 and 1 g/L graphene oxide, pH 2.5	Graphene oxide (GO)-containing zinc phosphate	4.65 ± 0.45 μm	Hank's solution	0.0685 ± 0.003						[190]
	Organic and polymer coating	Pure Zn (99.99+%)	Dip-coating in the 1 mg/ml rat tail type I collagen solution for 20 min at room temperature	Rat tail type I collagen	2.5 μm	Hank's solution	0.085 ± 0.009		i. Murine calvarial pre-osteoblast (MC3T3-E1) ii. Human endothelial cell (EA. hy926)	Improved cell proliferation and differentiation Improved cell proliferation	Platelets activation on the surface with hemolysis rate below 5%		[136]
	Biomimetic deposition	Zn-1.5Mg	Immersing in SBF for two weeks	Calcium phosphate		MEM cultivation medium with 5% fetal bovine serum		0.019 ± 0.011 (mg cm^{-2} day^{-1}, with CO_2 atmosphere); 0.004 ± 0.002 (mg cm^{-2} day^{-1}, without CO_2 atmosphere);	i. Murine fibroblast (L929) ii. Human osteosarcoma cell (U-2 OS)	Improved cell viability Improved cell adhesion number with more spreading			[155]
		Zn–3Cu–1Mg	Immersing in Ca $(H_2PO_4)\cdot H_2O$, sodium nitrate and hydrogen peroxide mixture solution for 1d at 20 °C	$CaHPO_4\cdot 2H_2O$					Bone marrow mesenchymal stem cell (BMSC)	Improved cell proliferation, osteogenic differentiation and calcium deposition			[191]
	Stabilization treatment	Zn–1Mg Zn–1Mg-0.5Ca	Immersing in Dulbecco's Modified Eagle's Medium for 1 day under a humidified atmosphere with 5% CO_2 at 37 °C	ZnO and Zn $(OH)_2$					Murine mesenchymal stem cell (MSC)	Improved cell adhesion and proliferation Improved cell adhesion and proliferation			[192]
Electrochemical method	Microarc oxidation	Pure Zn (99.999%)	400 V, 3 min, electrolyte: 2.5 g/L sodium hydroxide and 0.02 mol/L calcium	Zn and amorphous $Ca_3(PO_4)_2$	~25 μm	Hank's solution	1.361 ± 0.124		Human osteoblast-like cell (MG63)	Decreased cell proliferation and improved cell adhesion.			[137]

(*continued on next page*)

Table 5 (*continued*)

Surface modification method		Substrate	Techniques and modified layer	Main layer structure	Layer thickness	*In vitro* corrosion rate (mm/y)			*In vitro* biocompatibility			*In vivo* Biocompatibility	Ref.
						Corrosion medium	Electrochemical test	Immersion test	Cell line	Cytocompatibility	Hemocompatibility		
			glycerophosphate hydrate dissolved in deionized water										
Physical method	Atomic layer deposition	Zn-0.1Li	Tetrakis (dimethylamino) zirconium (TDMAZ) as Zr precursor (heated to 120 °C), deionized water as O precursor (heated to 35 °C), 500 deposition cycles	Amorphous ZrO_2	~120 nm	Hank's solution	0.054 ± 0.014		Murine osteoblast precursor cell (MC3T3-E1)	Improved cell adhesion and proliferation		Improved *in vivo* osseointegration	[135]
	Magnetron sputtering	Pure Zn (≥99.995%)	Target: high purity C, chamber pressure: 8 mTorr, Ar flow rate: 20 sccm, direct-current power: 90 V, deposition time:60 min	Diamond-like carbon	~100 nm				Murine osteoblast precursor cell (MC3T3-E1)	Decreased cell proliferation	Hemolysis rate was below 5%		[193]
Mechanical method	Sandblasting	Pure Zn	Abrasive: Al_2O_3 (250 μm particle size), distance between jet and sample surface: 10 mm, pressure: 2 bar, time: 20 s			DMEM/F-12		~0.035	Human osteosarcoma cell (Saos-2)	Decreased cell proliferatiom			[194]

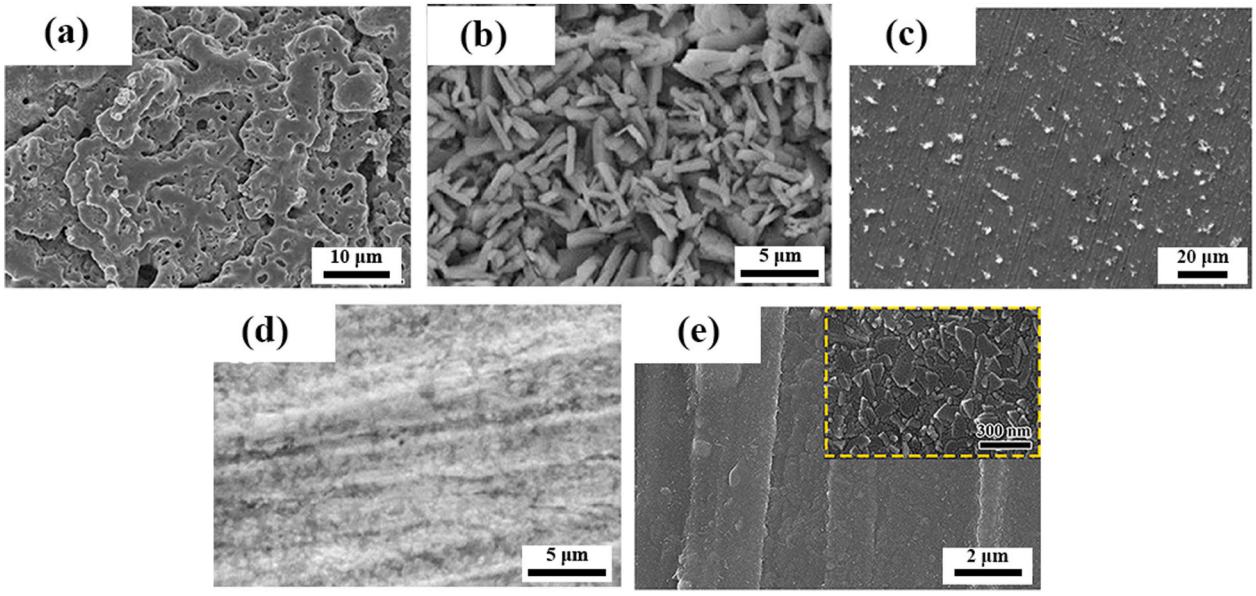

Fig. 7. The representative surface morphologies of the coatings prepared by different surface modification methods of Zn-based BMs for orthopedic application: (a) Microarc oxidation coating. (Reproduced with permissions from Ref. [137]). (b) Phosphate conversion coating. (Reproduced with permissions from Ref. [136]). (c) Biomimetic deposition. (Reproduced with permissions from Ref. [155]). (d) Collagen coating. (Reproduced with permissions from Ref. [136]). (e) Atomic layer deposition of ZrO_2 coating. (Reproduced with permissions from Ref. [135]).

surface of pure Zn. They found that the DLC film accelerated the corrosion of substrate, which is possibly attributed to the galvanic corrosion between the film and Zn substrate. Meanwhile, a decrease in cytocompatibility was also demonstrated for the DLC-coated Zn.

(7) Sandblasting

Sandblasting is a simple and universal approach to increase the surface roughness by forcing small grits of specific shape and size across the surface of materials [219,220]. In addition, it is also claimed that sandblasting can improve the biocompatibility of biomaterials by adjusting the surface roughness and morphology. Li et al. [194] investigated the effects of sandblasting surface treatment on degradation

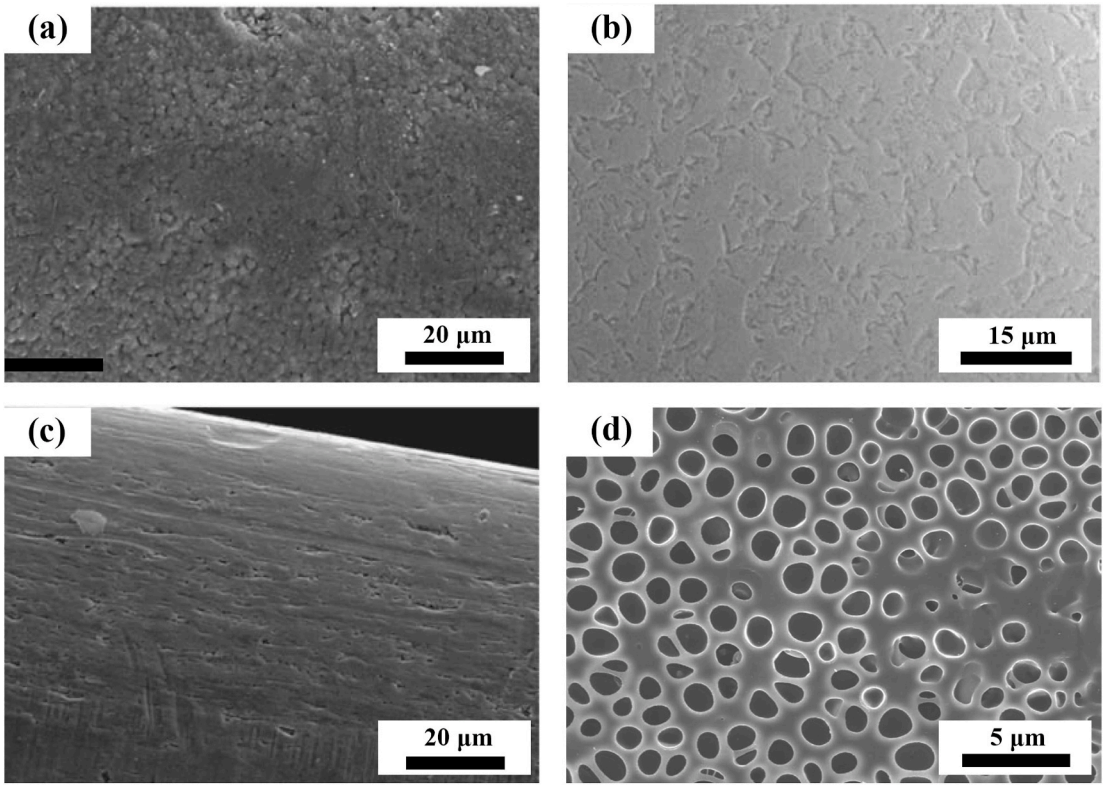

Fig. 8. The surface morphologies of the coatings prepared by different surface modification methods of Zn-based BMs for cardiovascular applications: (a) Anodization coating. (Reproduced with permissions from Ref. [223]). (b) Electropolished surface (Reproduced with permissions from Ref. [223]). (c) Air oxidation coating (Reproduced with permissions from Ref. [223]). (d) PLLA coating. (Reproduced with permissions from Ref. [222]).

behavior and biocompatibility of pure Zn, Zn–4Ag and Zn–2Ag-1.8Au-0.2 V. They found that sandblasting increased the corrosion rates of Zn and Zn alloys, while an adverse impact of sandblasting on cytocompatibility was also observed.

3.2. Surface modification of Zn-based BMs for cardiovascular applications

So far, there is only limited research on the surface modification of Zn-based BMs aimed at cardiovascular applications as summarized in Fig. 8 and Table 6. Shearier et al. [221] constructed dopamine coating and dopamine/gelatin composite coating on the surface of pure Zn foils. It was demonstrated that both coatings had a beneficial effect on the cell viability of human dermal fibroblasts, human aortic smooth muscle cells and human aortic endothelial cells. Shomali et al. [222] reported the preparation of MPS/PLLA coating on the surface of pure Zn wires by dip-coating. Although an improved corrosion resistance was achieved after surface modification, the biocompatibility was reduced with increased cytotoxicity and neointimal hyperplasia, which can be caused by the toxic and acid degradation by-products of PLLA. Drelich et al. [223] constructed oxide films of diverse thickness and structure on pure Zn wires by oxidation, electropolishing and anodization, and studied the impact of oxide films on the corrosion behavior. It is claimed that the defects/cracks in the oxide film will accelerate the biocorrosion of Zn-based BMs as local corrosion sites. MAO coating, which is mainly composed of ZnO and Zn_2SiO_4, was prepared on Zn–1Mg alloy by Sheng et al. [224]. A beneficial effect of MAO treatment on the corrosion resistance was observed. Besides, they also demonstrated improved

Table 6
Summary of different surface modification methods of biodegradable Zn-based BMs for cardiovascular applications.

Surface modification method	Substrate	Techniques and modified layer	Main layer structure	Layer thickness	Efficiency of the coating	Ref.
Organic coating	Pure Zn (99.9%)	Immersing in MPS for 30 min followed by dip-coating in PLLA solution at room temperature.	PLLA	1–12 μm	Increased corrosion resistance *in vitro* and *in vivo*. Decreased cytocompatibility with signs of toxicity and active neointima.	[222]
	Pure Zn foil (99.9%)	Immersing in the 2 mg/ml dopamine solution for 12 h.	Polydopamine		Improved cell viability of human dermal fibroblasts, human aortic smooth muscle cells and human aortic endothelial cells.	[221]
	Pure Zn foil (99.9%)	Zn foils were incubated in the 2 mg/ml dopamine solution for 12 h. A 100 μm-thickness section of gelatin was produced, and affixed to the dopamine-coated Zn foil by bringing them into contact. Gelatin-covered foils were then immersed in 10 mM EDC in 90% ethanol for 20 min to cross-link the gelatin.	Polydopamine/gelatin		Improved cell viability of human dermal fibroblasts, human aortic smooth muscle cells and human aortic endothelial cells.	[221]
	Zn–1Mg	Zn–1Mg plates were immersed in 1 mol/L NaOH solution for 0.5 h at 60 °C. Then, they were immersed in 2 mL silane hydrolysate solution for 12 h at 37 °C. Next, the samples were immersed in 2 mL of 1 mol/L glutaraldehyde for 12 h at 37 °C. Finally, they were immersed in 2 mg/ml phosphorylcholine chitosan copolymer solution for 12 h.	APTES/ phosphorylcholine chitosan copolymer		Increased corrosion resistance. Excellent hemocompatibility with hemolysis rate below 0.2%. Improved cell attachment and proliferation of human umbilical vein endothelial cells.	[225]
Air oxidation	Pure Zn wire (>99.99%)	350 °C for 1 and 2 h in a regular furnace in air.	ZnO	0.3–1.4 μm		[223]
Electropolishing	Pure Zn wire (>99.99%)	0.25 A/cm^2, 10 V, 2 min, electrolyte: 885 ml ethanol, 100 ml butanol, 109 g $AlCl_3{\cdot}6H_2O$, 250 g $ZnCl_2$, 120 ml H_2O.		0.06–0.08 (+0.05–0.15) μm		[223]
	Pure Zn (99.99%)	0.45 A, ~90s, electrolyte: 885 m L C_2H_5OH, 100 mL C_4H_9OH, 109 g $AlCl_3{\cdot}6H_2O$, 250 g $ZnCl_2$.			A 22% failure rate *in vivo* (2 out of 9 samples), with 44% of the observations meeting the full biocompatibility benchmarks.	[226]
Anodization	Pure Zn wire (>99.99%)	I. Electropolishing: 0.25 A/cm^2, 10 V, 2 min, electrolyte: 885 ml ethanol, 100 ml butanol, 109 g $AlCl_3{\cdot}6H_2O$, 250 g $ZnCl_2$, 120 ml H_2O. II. Anodization ~4 A, 10 V, 1 min, electrolyte: 1 L oxalic acid (0.1, 0.3 or 0.5 M) solution.	ZnO	5–10 μm		[223]
	Pure Zn (99.99%)	I. Electropolishing: 0.45 A, ~90s, electrolyte: 885 m L C_2H_5OH, 100 mL C_4H_9OH, 109 g $AlCl_3{\cdot}6H_2O$, 250 g $ZnCl_2$. II. Anodization: ~4 A, 1min, electrolyte: 0.5 M $(COOH)_2$.			100% of the treated samples (9 out of 9) met the full biocompatibility benchmarks *in vivo*, leading to a failure rate of 0% (0 out of 9).	[226]
Microarc oxidation	Zn-0.1Mg	300 V, 120 s, electrolyte: 14 g/L Na_2SiO_3, 2 g/L KOH, 15 ml/L glycol and 10 ml/L glycerol.	ZnO and Zn_2SiO_4	28.6 ± 2 μm	Improved blood compatibility with decreased hemolysis rate, lower lytic activity against red blood cells and lower platelet adhesion. Improved adhesion and viability of human umbilical vein endothelial cells.	[224]

blood compatibility and cytocompatibility of human umbilical vein endothelial cells after MAO treatment.

4. Perspectives on the future surface modification strategies of Zn-based BMs

4.1. Potential surface modification methods of Zn-based BMs for orthopedic applications

Surface modification on BMs, such as Mg- and Fe-based alloys, has been extensively investigated in order to adjust their corrosion behavior without causing any damage to the bulk attributes. In terms of Mg-based BMs, the aim of the surface modification mainly focuses on the down regulation of the corrosion rate, alleviating the related complications caused by the rapid corrosion simultaneously [227,228]. In contrast, the surface modification on Fe-based BMs holds the opposite purpose [229, 230]. Nonetheless, it seems that the demand of surface modification of Zn-based BMs for orthopedic applications stems from two issues based on the present research results, namely susceptible biocompatibility and retarded corrosion behavior. Firstly, excessive release of Zn ions can lead to an undesired biological response including *in vitro* cytotoxicity and *in vivo* delayed osseointegration despite a much lower ion concentration than that of Mg and Fe, as discussed above. Secondly, although Zn is featured by the more appropriate corrosion rate compared with Mg and Fe, it seems that the *in vivo* corrosion rates of Zn-based BMs are relatively slow in orthopedic environment (Table 2). From these perspectives, diverse surface modification methods can be taken into account to tackle the problems (Fig. 9).

4.1.1. Surface modification methods of accelerating biodegradation of Zn-based BMs

(1) Metallic elements ion implantation

Ion implantation can incorporate specific ions within the atomic network of surface without altering the bulk materials attributes [231]. Previous study has demonstrated that alloying Zn with IIA elements, such as Mg, Ca and Sr can improve the biocompatibility and accelerate the corrosion rates [132]. Yang et al. [145] also claimed that incorporating Mg into Zn matrix as sacrificial anode showed a beneficial effect on the *in vitro* and *in vivo* biocompatibility with decreased corrosion resistance. Such improved biocompatibility was attributed to the synergistic release of Zn^{2+} and Mg^{2+}. Hence, it is hypothesized that incorporation of IIA elements on the surface of Zn-based BMs by ion implantation could improve the biocompatibility along with an increase in the corrosion rate.

(2) Polymer-based coatings

When served in the physiological environment, some polymer coatings such as PLA, PLGA and PDLLA degrade and release acidic degradation products [232]. The resultant local acidic environment is

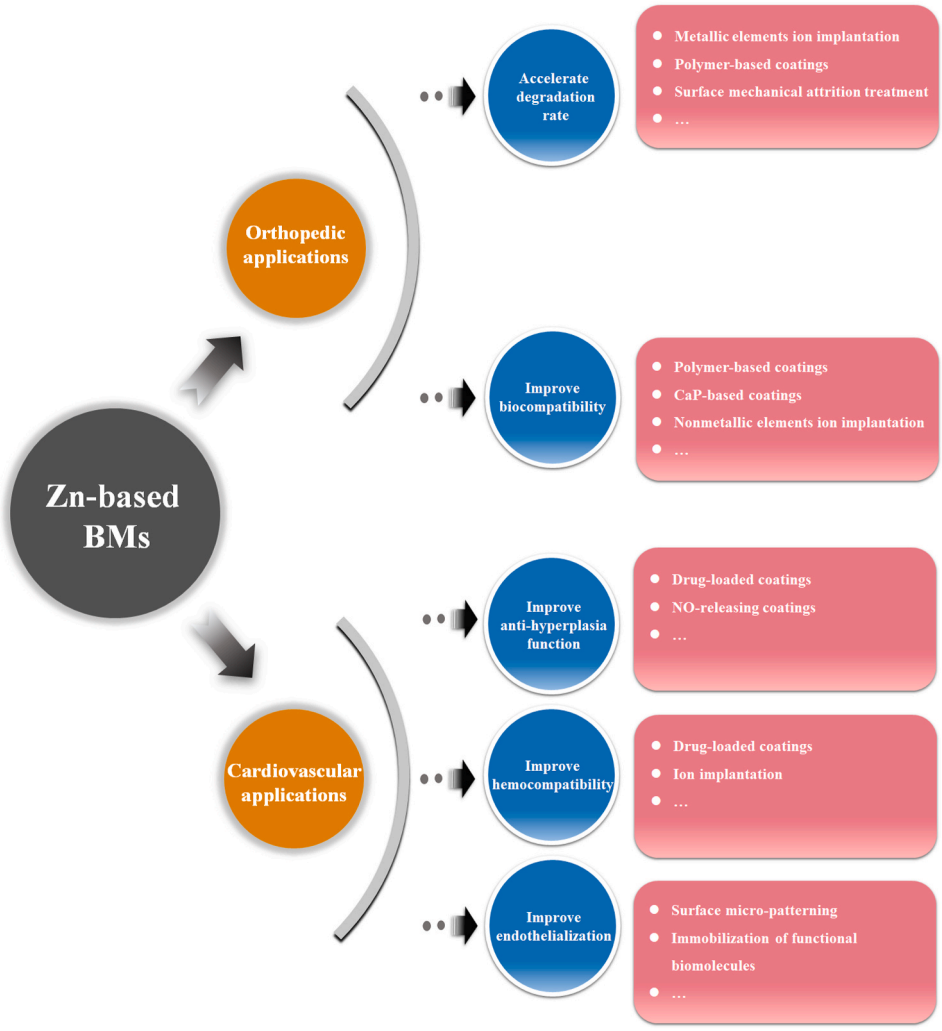

Fig. 9. The future perspectives of surface modification of Zn-based BMs for orthopedic and cardiovascular applications.

expected to accelerate the corrosion of underlying BMs. Lin et al. [233] developed a layer of PDLLA coating on iron-based coronary scaffolds and successfully shortened the corrosion period of stent due to the formation of local acidic environment. Similar phenomenon of expedited corrosion has also been demonstrated by Yusop et al. when infiltrating PLGA into porous iron [234].

(3) Surface mechanical attrition treatment

Surface mechanical attrition treatment (SMAT) is one of the severe plastic deformation methods which can refine the grain size of treated metal surface to nanoscale. Meanwhile, the grain refinement and the interaction of dislocations after SMAT will bring about an improvement in the mechanical properties [235]. In addition, the increased surface roughness as well as high density of crystalline defects and micro cracks will impair the corrosion resistance of treated alloys, resulting in accelerated degradation behavior [236,237].

4.1.2. Surface modification methods of improving the biocompatibility of Zn-based BMs

(1) polymer-based coatings

Degradable natural polymers (e.g. chitosan, collagen and silk fibroin) have been widely applied on the surface of Mg-based BMs to improve their corrosion resistance and biocompatibility [232,238]. They can serve as physical barriers isolating the underlying metals from corrosive media [239]. Meanwhile, no acid degradation products will be released during degradation process. In addition, other functionalities, including self-healing [238], anti-inflammation [240] and osteoinduction [241], can also be achieved when loaded with functional agents.

(2) CaP-based coatings

Calcium phosphate (CaP) is the primary inorganic component in about 60% of native human bones [242]. Due to its superior biocompatibility and bioactivity, CaP has been intensively studied in the orthodontics and orthopedics as bone substitutes [243]. It shows a beneficial effect on the bone formation and generates chemical bonding to the newly-formed bone [244]. Recently, much attention has been focused on the application of CaP as coating material on the surface of Mg-based BMs for corrosion protection and biocompatibility improvement [245–248]. Diverse methods have been conducted to construct CaP coating on Mg-based BMs such as sol-gel [249], electrodeposition [250], hydrothermal deposition [251], pulsed laser deposition [252] and so on. Previous study has demonstrated that incorporating hydroxyapatite into Zn can significantly improve the *in vivo* osteogenesis [146]. Therefore, CaP coatings can be promising approach to improve the biocompatibility of Zn-based BMs with minimal effect on the bulk attributes.

(3) Nonmetallic elements ion implantation

The incorporation of nonmetallic elements (O, C, H, N, P, S, F, Si, and Se) into the surface of Zn-based BMs can also be considered on account of their high content in human body [108]. For instance, it is claimed that hydrated zinc phosphate is thermodynamically preferred in physiologically aqueous environment. Meanwhile, zinc phosphate coating has shown a stimulative impact on the biocompatibility of pure Zn [136]. Therefore, it is suggested that P ion implantation may improve the biocompatibility of Zn-based BMs by interaction of phosphate ions and released Zn ions in addition to the abundant existence and physiological functions of P in bone tissue.

Nevertheless, a blind increase in the corrosion resistance of Zn-based BMs after constructing physical barrier may compromise their advantages on the corrosion behaviors and result in a longer retention of implants despite an improvement in biocompatibility. Therefore, controversies have been aroused on the current surface modification methods of Zn-based BMs in orthopedic environment, dedicating efforts to intently improve the corrosion resistance. Generally speaking, controllable corrosion rate, either decreased or accelerated, should be under consideration based on outcomes of the healing process of injured tissue. In this way, composite coatings involving different surface modification methods should be developed. The design of a "smart" coating, which can alleviate the toxic influence of Zn^{2+} and exploit the advantages of the degradation behavior of bulk materials, is expected in the future development of surface modification techniques of Zn-based BMs.

4.2. Potential surface modification methods of Zn-based BMs for cardiovascular applications

On the basis of the present research, Zn-based BMs shows the near-ideal *in vivo* corrosion behavior in cardiovascular environment. However, in spite of significant improvement of the mechanical properties compared with pure Zn, some alloy systems show signs of intimal activation with mild inflammation as discussed above. Meanwhile, the current implantation sites for the *in vivo* experiments are limited to the healthy blood vessels, which might result in a different healing process in comparison with that of lesioned vessels. Therefore, pathological models should be adopted to further verify the *in vivo* biocompatibility of Zn-based BMs. In terms of the clinical requirements, the cardiovascular implants should possess anti-hyperplasia function, hemocompatibility and re-endotheliallization ability [253]. Herein, some potential and promising surface modification methods of Zn-based BMs for further cardiovascular applications have been put forward according to the clinical requirements, as shown in Fig. 9.

4.2.1. Surface modification methods of improving the anti-hyperplasia function of Zn-based BMs

(1) Drug-loaded coatings

Some antiproliferative drugs or inhibitors, such as paclitaxel [254], sirolimus [255], rapamycin [256] TNF-α antibody [257] and so on, are able to suppress the intimal hyperplasia. Meanwhile, such drug molecules can be incorporated into the polymer coatings to improve the anti-hyperplasia function. It is found that paclitaxel-loaded biodegradable film made of chondroitin sulfate and gelatin can reduce the neointima formation [258]. Besides, Shi et al. [259] prepared rapamycin-eluting PDLLA coating on Mg alloy. It is claimed that the modified stents exhibited favorable biosafety with comparable neointima formation to the commercial non-degradable drug-eluting stents.

(2) NO-releasing coatings

Nitric oxide (NO) plays an important role in the regulation of intimal hyperplasia. It can suppress the proliferation and migration of vascular smooth muscle cell (VSMC), stimulate the apoptosis of VSMC and inhibit leukocyte chemotaxis [260]. NO-releasing coatings have been utilized to prevent restenosis. Zhang et al. [261] constructed dopamine/Cu ion biomimetic coating on stainless steel stent. The biomimetic coating can generate NO locally and reduced neointimal formation *in vivo*.

4.2.2. Surface modification methods of improving the hemocompatibility of Zn-based BMs

(1) Drug-loaded coatings

Several drugs and biomolecules such as herapin [262], phosphorylcholine [263], and albumin [264] can be used in the surface modification of stent to improve the blood compatibility. Lee et al. [265]

constructed heparin coating on the 3D printed PLA stents. It is found that heparin coating improved the hemocompatibility with reduced fibrinogen and platelet adhesion.

(2) ion implantation

Fe–O film have been applied on the surface of pure Fe via plasma immersion ion implantation. The Fe–O film showed favorable hemocompatibility with only slight platelet activation [266]. Besides, it is also reported that incorporating Lanthanum (La) and Helium (He) into the surface had a beneficial effect on the blood compatibility. Zhu et al. [267] implanted La ion into pure Fe and demonstrated an improved hemocompatibility with decreased platelets adhesion, activation, aggregation and pseudopodium. In addition, Sugita et al. [268] implanted He ion into the collagen-coated Ti–Ni stents and exhibited excellent antithrombogenicity compared with the non-implanted collagen-coated stents.

4.2.3. Surface modification methods of improving endothelialization of Zn-based BMs

(1) Surface micro-patterning

Surface topography plays a significant role in the regulation of cellular cues including cell size, shape, adhesion, migration and proliferation [269]. The endothelial cell shape, which will influence the cell functions, can be controlled by surface micro-patterning independent of external forces [270]. Liang et al. [271] prepared biomimetic surface pattern based on the morphology of vascular smooth muscle cells on 316 L cardiovascular stent by femtosecond laser. A beneficial effect was found on the *in vitro* adhesion, proliferation and migration of endothelial cells as well as the *in vivo* re-endothelialization.

(2) Immobilization of functional biomolecules

Constructing functional coatings consisting of biomolecules such as REDV peptide [272], vascular endothelial growth factor (VEGV) [273], heparin [274] and anti-CD34 antibody [275] will have a beneficial impact on the re-endothelialization. Aoki et al. [276] demonstrated immobilization of CD34 antibody on stainless steel stent resulted in an accelerated re-endothelialization owning to the capture of endothelial progenitor cells.

5. Conclusions

In the past few years, Zn and its alloys have gained great interest as BMs owning to their favorable corrosion behavior and acceptable biocompatibility, following after Mg- and Fe-based BMs. However, in comparison with years of research and application in industrial field, the research of biomedical Zn-based materials is still in the initial stage. In this review, the state of the art of bulk Zn-based BMs and relevant surface modification strategies have been comprehensively summarized from the aspects of orthopedic and cardiovascular applications. Note that the previous surface modifications on Zn are mainly focused on the industrial applications regardless of the biosafety and degradation period, the challenges and future development directions of surface modification of Zn-based BMs for biomedical applications have also been discussed:

(1) In terms of orthopedic applications, the recently-developed Zn-based BMs exhibit dilatory corrosion in physiological environment. Besides, the low concentration threshold of Zn ion for cells and tissues also remains a concern. From this point of view, endeavor should be made to achieve accelerated degradation and controllable release of degradation products simultaneously. Therefore, various potential surface modification techniques have been proposed based on these two issues such as polymer-based coating, ion implantation and so on. Meanwhile, in contrast with one-way adjustment of corrosion behavior for the surface modification of Mg- and Fe-based BMs, composite coatings fabricated by the combination of different surface modification methods can be taken into account for Zn-based BMs to adjust the corrosion behavior and enhance the bone formation ability simultaneously.

(2) When it comes to the cardiovascular applications, some Zn-based BMs exhibited intimal activation with mild inflammation, which may impair the therapeutic effect of implanted devices. Meanwhile, the current implantation sites of Zn-based BMs are limited to the healthy blood vessels. Hence, further researches should be focused on the host response to the Zn-based BMs after being implanted in the pathological vessels in the future. Besides, in order to further improve the performance of Zn-based BMs, some potential surface modification technologies have been put forward to enhance the anti-hyperplasia function, hemocompatibility and re-endothelialization such as the drug-loaded coatings, ion implantation, surface micro-patterning and so on.

Declaration of competing interest

The authors declared that they have no conflicts of interest to this paper. We declare that we do not have any commercial or associative interest that represents a conflict of interest in connection with this paper.

Acknowledgements

This work was supported by the National Natural Science Foundation of China (Grant No. 51931001, 51901003), the International Cooperation and Exchange project between NSFC (China) and CNR (Italy) (NSFC-CNR Grant No. 52011530392), the Open Project of NMPA Key Laboratory for Dental Materials (Grant No. PKUSS20200401).

References

[1] D. Apelian, M. Paliwal, D.C. Herrschaft, Casting with zinc alloys, JMET (J. Med. Eng. Technol.) 33 (11) (1981) 12–20.
[2] M.T. Abou El-khair, A. Daoud, A. Ismail, Effect of different Al contents on the microstructure, tensile and wear properties of Zn-based alloy, Mater. Lett. 58 (11) (2004) 1754–1760.
[3] J.B. Bajat, V.B. Mišković-Stanković, N. Bibić, D.M. Dražić, The influence of zinc surface pretreatment on the adhesion of epoxy coating electrodeposited on hot-dip galvanized steel, Prog. Org. Coating 58 (4) (2007) 323–330.
[4] M.A. Arenas, C. Casado, V. Nobel-Pujol, J. Damborenea, Influence of the conversion coating on the corrosion of galvanized reinforcing steel, Cement Concr. Compos. 28 (3) (2006) 267–275.
[5] M. Fedel, M. Poelman, M. Olivier, F. Deflorian, Sebacic acid as corrosion inhibitor for hot-dip galvanized (HDG) steel in 0.1 M NaCl, Surf. Interface Anal. 51 (5) (2019) 541–551.
[6] S.M.A. Shibli, B.N. Meena, R. Remya, A review on recent approaches in the field of hot dip zinc galvanizing process, Surf. Coating. Technol. 262 (2015) 210–215.
[7] R.B. Figueira, C.J.R. Silva, E.V. Pereira, Hybrid sol–gel coatings for corrosion protection of galvanized steel in simulated concrete pore solution, J. Coating Technol. Res. 13 (2) (2016) 355–373.
[8] N. Pistofidis, G. Vourlias, D. Chaliampalias, K. Chrysafis, G. Stergioudis, E. K. Polychroniadis, On the mechanism of formation of zinc pack coatings, J. Alloys Compd. 407 (1–2) (2006) 221–225.
[9] P.R. Seré, M. Banera, W.A. Egli, C.I. Elsner, A.R. Di Sarli, C. Deyá, Effect on temporary protection and adhesion promoter of silane nanofilms applied on electro-galvanized steel, Int. J. Adhesion Adhes. 65 (2016) 88–95.
[10] Z.I. Ortiz, P. Díaz-Arista, Y. Meas, R. Ortega-Borges, G. Trejo, Characterization of the corrosion products of electrodeposited Zn, Zn–Co and Zn–Mn alloys coatings, Corrosion Sci. 51 (11) (2009) 2703–2715.
[11] R. Ramanauskas, P. Quintana, L. Maldonado, R. Pomés, M. Pech-Canul, Corrosion resistance and microstructure of electrodeposited Zn and Zn alloy coatings, Surf. Coating. Technol. 92 (1–2) (1997) 16–21.
[12] G. Tian, M. Zhang, Y. Zhao, J. Li, H. Wang, X. Zhang, H. Yan, High Corrosion protection performance of a novel nonfluorinated biomimetic superhydrophobic Zn-Fe coating with echinopsis multiplex-like structure, ACS Appl. Mater. Interfaces 11 (41) (2019) 38205–38217.

[13] X. Zhang, C. van den Bos, W.G. Sloof, A. Hovestad, H. Terryn, J.H.W. de Wit, Comparison of the morphology and corrosion performance of Cr(VI)- and Cr(III)-based conversion coatings on zinc, Surf. Coating. Technol. 199 (1) (2005) 92–104.

[14] H.Y. Su, C.S. Lin, Effect of additives on the properties of phosphate conversion coating on electrogalvanized steel sheet, Corrosion Sci. 83 (2014) 137–146.

[15] S. Zhang, B. Yang, G. Kong, J. Lu, Electrochemical analysis of molybdate conversion coating on hot-dip galvanized steel in various growth stages, Surf. Interface Anal. 49 (8) (2017) 698–704.

[16] Z. Zou, N. Li, D. Li, H. Liu, S. Mu, A vanadium-based conversion coating as chromate replacement for electrogalvanized steel substrates, J. Alloys Compd. 509 (2) (2011) 503–507.

[17] J. Min, J.H. Park, H.K. Sohn, J.M. Park, Synergistic effect of potassium metal siliconate on silicate conversion coating for corrosion protection of galvanized steel, J. Ind. Eng. Chem. 18 (2) (2012) 655–660.

[18] G. Kong, L. Lingyan, J. Lu, C. Che, Z. Zhong, Corrosion behavior of lanthanum-based conversion coating modified with citric acid on hot dip galvanized steel in aerated 1M NaCl solution, Corrosion Sci. 53 (4) (2011) 1621–1626.

[19] C. Motte, M. Poelman, A. Roobroeck, M. Fedel, F. Deflorian, M.G. Olivier, Improvement of corrosion protection offered to galvanized steel by incorporation of lanthanide modified nanoclays in silane layer, Prog. Org. Coating 74 (2) (2012) 326–333.

[20] I.A. Kartsonakis, A.C. Balaskas, E.P. Koumoulos, C.A. Charitidis, G.C. Kordas, Incorporation of ceramic nanocontainers into epoxy coatings for the corrosion protection of hot dip galvanized steel, Corrosion Sci. 57 (2012) 30–41.

[21] P. Wan, L. Tan, K. Yang, Surface modification on biodegradable magnesium alloys as orthopedic implant materials to improve the bio-adaptability: a review, J. Mater. Sci. Technol. 32 (9) (2016) 827–834.

[22] J. Wang, J. Tang, P. Zhang, Y. Li, J. Wang, Y. Lai, L. Qin, Surface modification of magnesium alloys developed for bioabsorbable orthopedic implants: a general review, J. Biomed. Mater. Res., Part B 100 (6) (2012) 1691–1701.

[23] H. Hornberger, S. Virtanen, A.R. Boccaccini, Biomedical coatings on magnesium alloys - a review, Acta Biomater. 8 (7) (2012) 2442–2455.

[24] M.P. Gigandet, J. Faucheu, M. Tachez, Formation of black chromate conversion coatings on pure and zinc alloy electrolytic deposits: role of the main constituents, Surf. Coating. Technol. 89 (3) (1997) 285–291.

[25] T. Bellezze, G. Roventi, R. Fratesi, Electrochemical study on the corrosion resistance of Cr III-based conversion layers on zinc coatings, Surf. Coating. Technol. 155 (2–3) (2002) 221–230.

[26] J. Zhao, L. Xia, A. Sehgal, D. Lu, R.L. McCreery, G.S. Frankel, Effects of chromate and chromate conversion coatings on corrosion of aluminum alloy 2024-T3, Surf. Coating. Technol. 140 (1) (2001) 51–57.

[27] M.R. Yuan, J.T. Lu, G. Kong, C.S. Che, Self healing ability of silicate conversion coatings on hot dip galvanized steels, Surf. Coating. Technol. 205 (19) (2011) 4507–4513.

[28] C. Barnes, J.J.B. Ward, T.S. Sehmbhi, V.E. Carter, Non-chromate passivation treatments for zinc, Trans. IMF 60 (1) (2017) 45–48.

[29] N.T. Wen, C.S. Lin, C.Y. Bai, M.D. Ger, Structures and characteristics of Cr(III)-based conversion coatings on electrogalvanized steels, Surf. Coating. Technol. 203 (3–4) (2008) 317–323.

[30] Y.T. Chang, N.T. Wen, W.K. Chen, M.D. Ger, G.T. Pan, T.C.K. Yang, The effects of immersion time on morphology and electrochemical properties of the Cr(III)-based conversion coatings on zinc coated steel surface, Corrosion Sci. 50 (12) (2008) 3494–3499.

[31] T. Bellezze, G. Roventi, R. Fratesi, Electrochemical study on the corrosion resistance of Cr III-based conversion layers on zinc coatings, Surf. Coating. Technol. 155 (2–3) (2002) 221–230.

[32] K. Cho, V. Shankar Rao, H. Kwon, Microstructure and electrochemical characterization of trivalent chromium based conversion coating on zinc, Electrochim. Acta 52 (13) (2007) 4449–4456.

[33] B. Ramezanzadeh, M.M. Attar, M. Farzam, Corrosion performance of a hot-dip galvanized steel treated by different kinds of conversion coatings, Surf. Coating. Technol. 205 (3) (2010) 874–884.

[34] D. Weng, P. Jokiel, A. Uebleis, H. Boehni, Corrosion and protection characteristics of zinc and manganese phosphate coatings, Surf. Coating. Technol. 88 (1–3) (1996) 147–156.

[35] D. Zimmermann, A.G. Muñoz, J.W. Schultze, Formation of Zn–Ni alloys in the phosphating of Zn layers, Surf. Coating. Technol. 197 (2–3) (2005) 260–269.

[36] M. Wolpers, J. Angeli, Activation of galvanized steel surfaces before zinc phosphating — XPS and GDOES investigations, Appl. Surf. Sci. 179 (1–4) (2001) 281–291.

[37] V. de Freitas Cunha Lins, G.F. de Andrade Reis, C.R. de Araujo, T. Matencio, Electrochemical impedance spectroscopy and linear polarization applied to evaluation of porosity of phosphate conversion coatings on electrogalvanized steels, Appl. Surf. Sci. 253 (5) (2006) 2875–2884.

[38] P.E. Tegehall, The mechanism of chemical activation with titanium phosphate colloids in the formation of zinc phosphate conversion coatings, Colloids Surf., A 49 (1990) 373–383.

[39] P.E. Tegehall, Colloidal titanium phosphate, the chemical activator in surface conditioning before zinc phosphating, Colloids Surf., A 42 (1) (1989) 155–164.

[40] C.Y. Tsai, J.S. Liu, P.L. Chen, C.S. Lin, Effect of Mg^{2+} on the microstructure and corrosion resistance of the phosphate conversion coating on hot-dip galvanized sheet steel, Corrosion Sci. 52 (12) (2010) 3907–3916.

[41] K. Ishizuka, K. Hayashi, H. Shindo, K. Nishimura, The effect of Mg addition to the phosphate film on the properties of prephosphated electrogalvanized steel sheets, Galvanotechnik (2007) 219–223.

[42] N. Satoh, Effects of heavy metal additions and crystal modification on the zinc phosphating of electrogalvanized steel sheet, Surf. Coating. Technol. 30 (2) (1987) 171–181.

[43] A.S. Akhtar, D. Susac, P. Glaze, K.C. Wong, P.C. Wong, K.A.R. Mitchell, The effect of Ni^{2+} on zinc phosphating of 2024-T3 Al alloy, Surf. Coating. Technol. 187 (2–3) (2004) 208–215.

[44] A.S. Akhtar, K.C. Wong, P.C. Wong, K.A.R. Mitchell, Effect of Mn^{2+} additive on the zinc phosphating of 2024-Al alloy, Thin Solid Films 515 (20–21) (2007) 7899–7905.

[45] B.L. Lin, J.T. Lu, G. Kong, Synergistic corrosion protection for galvanized steel by phosphating and sodium silicate post-sealing, Surf. Coating. Technol. 202 (9) (2008) 1831–1838.

[46] B.L. Lin, J.T. Lu, G. Kong, Effect of molybdate post-sealing on the corrosion resistance of zinc phosphate coatings on hot-dip galvanized steel, Corrosion Sci. 50 (4) (2008) 962–967.

[47] C.B. Breslin, G. Treacy, W.M. Carroll, Studies on the passivation of aluminium in chromate and molybdate solutions, Corrosion Sci. 36 (7) (1994) 1143–1154.

[48] K. Tanno, M. Itoh, H. Sekiya, H. Yashiro, N. Kumagai, The corrosion inhibition of carbon steel in lithium bromide solution by hydroxide and molybdate at moderate temperatures, Corrosion Sci. 34 (9) (1993) 1453–1461.

[49] K. Sugimoto, Y. Sawada, The role of alloyed molybdenum in austenitic stainless steels in the inhibition of pitting in neutral halide solutions, Corrosion 32 (9) (1976) 347–352.

[50] K. Aramaki, The inhibition effects of chromate-free, anion inhibitors on corrosion of zinc in aerated 0.5 M NaCl, Corrosion Sci. 43 (4) (2001) 591–604.

[51] G.D. Wilcox, D.R. Gabe, M.E. Warwick, The development of passivation coatings by cathodic reduction in sodium molybdate solutions, Corrosion Sci. 28 (6) (1988) 577–587.

[52] D.E. Walker, G.D. Wilcox, Molybdate based conversion coatings for zinc and zinc alloy surfaces: a review, Trans. IMF 86 (5) (2013) 251–259.

[53] A.A.O. Magalhães, I.C.P. Margarit, O.R. Mattos, Molybdate conversion coatings on zinc surfaces, J. Electroanal. Chem. 572 (2) (2004) 433–440.

[54] A. Nazarov, D. Thierry, T. Prosek, N.L. Bozecb, Protective action of vanadate at defected areas of organic coatings on zinc, J. Electrochem. Soc. 152 (7) (2005) B220.

[55] B.L. Hurley, K.D. Ralston, R.G. Buchheit, Corrosion inhibition of zinc by aqueous vanadate species, J. Electrochem. Soc. 161 (10) (2014) C471–C475.

[56] Z. Zou, N. Li, D. Li, Corrosion protection properties of vanadium films formed on zinc surfaces, Rare Met. 30 (2) (2011) 146–149.

[57] Z. Gao, D. Zhang, S. Jiang, Q. Zhang, X. Li, XPS investigations on the corrosion mechanism of V(IV) conversion coatings on hot-dip galvanized steel, Corrosion Sci. 139 (2018) 163–171.

[58] Z. Gao, D. Zhang, L. Hou, X. Li, Y. Wei, Understanding of the corrosion protection by V(IV) conversion coatings from a sol-gel perspective, Corrosion Sci. 161 (2019).

[59] Z. Gao, D. Zhang, X. Qiu, S. Jiang, Y. Wu, Q. Zhang, X. Li, The mechanisms of corrosion inhibition of hot-dip galvanized steel by vanadyl oxalate: a galvanic corrosion investigation supported by XPS, Corrosion Sci. 142 (2018) 153–160.

[60] M. Olivier, A. Lanzutti, C. Motte, L. Fedrizzi, Influence of oxidizing ability of the medium on the growth of lanthanide layers on galvanized steel, Corrosion Sci. 52 (4) (2010) 1428–1439.

[61] M. Machkova, E.A. Matter, S. Kozhukharov, V. Kozhukharov, Effect of the anionic part of various Ce(III) salts on the corrosion inhibition efficiency of AA2024 aluminium alloy, Corrosion Sci. 69 (2013) 396–405.

[62] S. Bernal, F.J. Botana, J.J. Calvino, M. Marcos, J.A. Pérez-Omil, H. Vidal, Lanthanide salts as alternative corrosion inhibitors, J. Alloys Compd. 225 (1–2) (1995) 638–641.

[63] L. Paussa, F. Andreatta, N.C. Rosero Navarro, A. Durán, L. Fedrizzi, Study of the effect of cerium nitrate on AA2024-T3 by means of electrochemical micro-cell technique, Electrochim. Acta 70 (2012) 25–33.

[64] B.R.W. Hinton, L. Wilson, The corrosion inhibition of zinc with cerous chloride, Corrosion Sci. 29 (8) (1989) 967–985.

[65] K. Aramaki, The inhibition effects of cation inhibitors on corrosion of zinc in aerated 0.5 M NaCl, Corrosion Sci. 43 (8) (2001) 1573–1588.

[66] K. Aramaki, Treatment of zinc surface with cerium(III) nitrate to prevent zinc corrosion in aerated 0.5 M NaCl, Corrosion Sci. 43 (11) (2001) 2201–2215.

[67] M.F. Montemor, A.M. Simões, M.G.S. Ferreira, Composition and behaviour of cerium films on galvanised steel, Prog. Org. Coating 43 (4) (2001) 274–281.

[68] M.A. Arenas, J.J. de Damborenea, Surface characterisation of cerium layers on galvanised steel, Surf. Coating. Technol. 187 (2–3) (2004) 320–325.

[69] M.F. Montemor, A.M. Simões, M.G.S. Ferreira, Composition and corrosion behaviour of galvanised steel treated with rare-earth salts: the effect of the cation, Prog. Org. Coating 44 (2) (2002) 111–120.

[70] K. Aramaki, A self-healing protective film prepared on zinc by treatment in a Ce$(NO_3)_3$ solution and modification with Ce$(NO_3)_3$, Corrosion Sci. 47 (5) (2005) 1285–1298.

[71] S.H. Zhang, G. Kong, J.T. Lu, C.S. Che, L.Y. Liu, Growth behavior of lanthanum conversion coating on hot-dip galvanized steel, Surf. Coating. Technol. 259 (2014) 654–659.

[72] G. Kong, L. Liu, J. Lu, C. Che, Z. Zhong, Study on lanthanum salt conversion coating modified with citric acid on hot dip galvanized steel, J. Rare Earths 28 (3) (2010) 461–465.

[73] D. Wang, X. Tang, Y. Qiu, F. Gan, G. Zheng Chen, A study of the film formation kinetics on zinc in different acidic corrosion inhibitor solutions by quartz crystal microbalance, Corrosion Sci. 47 (9) (2005) 2157–2172.

[74] M.R. Yuan, J.T. Lu, G. Kong, C.S. Che, Effect of silicate anion distribution in sodium silicate solution on silicate conversion coatings of hot-dip galvanized steels, Surf. Coating. Technol. 205 (19) (2011) 4466–4470.

[75] M. Hara, R. Ichino, M. Okido, N. Wada, Corrosion protection property of colloidal silicate film on galvanized steel, Surf. Coating. Technol. 169–170 (2003) 679–681.

[76] S.H. Zhang, G. Kong, Z.W. Sun, C.S. Che, J.T. Lu, Effect of formulation of silica-based solution on corrosion resistance of silicate coating on hot-dip galvanized steel, Surf. Interface Anal. 48 (3) (2016) 132–138.

[77] S. Dalbin, G. Maurin, R.P. Nogueira, J. Persello, N. Pommier, Silica-based coating for corrosion protection of electrogalvanized steel, Surf. Coating. Technol. 194 (2–3) (2005) 363–371.

[78] M.R. Yuan, J.T. Lu, G. Kong, Effect of SiO_2:Na_2O molar ratio of sodium silicate on the corrosion resistance of silicate conversion coatings, Surf. Coating. Technol. 204 (8) (2010) 1229–1235.

[79] F. Jamali, I. Danaee, D. Zaarei, Effect of nano-silica on the corrosion behavior of silicate conversion coatings on hot-dip galvanized steel, Mater. Corros. 66 (5) (2015) 459–464.

[80] V.A. Paramonov, A.T. Moroz, N.G. Filatova, O.A. Kazandzhiyan, Chromateless treatment of zinc-plated rolled metal, Protect. Met. 43 (3) (2007) 288–290.

[81] J.K. Chang, C.S. Lin, W.J. Cheng, I.H. Lo, W.R. Wang, Oxidation resistant silane coating for hot-dip galvanized hot stamping steel, Corros. Sci., 2019, p. e.

[82] M.L. Zheludkevich, R. Serra, M.F. Montemor, K.A. Yasakau, I.M.M. Salvado, M.G. S. Ferreira, Nanostructured sol–gel coatings doped with cerium nitrate as pre-treatments for AA2024-T3, Electrochim. Acta 51 (2) (2005) 208–217.

[83] M.F. Montemor, M.G.S. Ferreira, Analytical characterization of silane films modified with cerium activated nanoparticles and its relation with the corrosion protection of galvanised steel substrates, Prog. Org. Coating 63 (3) (2008) 330–337.

[84] M.F. Montemor, M.G.S. Ferreira, Cerium salt activated nanoparticles as fillers for silane films: evaluation of the corrosion inhibition performance on galvanised steel substrates, Electrochim. Acta 52 (24) (2007) 6976–6987.

[85] F. Brusciotti, A. Batan, I. De Graeve, M. Wenkin, M. Biessemans, R. Willem, F. Reniers, J.J. Pireaux, M. Piens, J. Vereecken, H. Terryn, Characterization of thin water-based silane pre-treatments on aluminium with the incorporation of nano-dispersed CeO_2 particles, Surf. Coating. Technol. 205 (2) (2010) 603–613.

[86] M.F. Montemor, W. Trabelsi, M. Zheludevich, M.G.S. Ferreira, Modification of bis-silane solutions with rare-earth cations for improved corrosion protection of galvanized steel substrates, Prog. Org. Coating 57 (1) (2006) 67–77.

[87] W. Trabelsi, P. Cecilio, M.G.S. Ferreira, M.F. Montemor, Electrochemical assessment of the self-healing properties of Ce-doped silane solutions for the pre-treatment of galvanised steel substrates, Prog. Org. Coating 54 (4) (2005) 276–284.

[88] O.D. Lewis, G.W. Critchlow, G.D. Wilcox, A. deZeeuw, J. Sander, A study of the corrosion resistance of a waterborne acrylic coating modified with nano-sized titanium dioxide, Prog. Org. Coating 73 (1) (2012) 88–94.

[89] M.F. Montemor, A.M. Cabral, M.L. Zheludkevich, M.G.S. Ferreira, The corrosion resistance of hot dip galvanized steel pretreated with Bis-functional silanes modified with microsilica, Surf. Coating. Technol. 200 (9) (2006) 2875–2885.

[90] A. Phanasgaonkar, V. Raja, Influence of curing temperature, silica nanoparticles-and cerium on surface morphology and corrosion behaviour of hybrid silane coatings on mild steel, Surf. Coating. Technol. 203 (16) (2009) 2260–2271.

[91] H. Liu, S. Szunerits, W. Xu, R. Boukherroub, Preparation of superhydrophobic coatings on zinc as effective corrosion barriers, ACS Appl. Mater. Interfaces 1 (6) (2009) 1150–1153.

[92] S. Heise, M. Höhlinger, Y.T. Hernández, J.J.P. Palacio, J.A. Rodriquez Ortiz, V. Wagener, S. Virtanen, A.R. Boccaccini, Electrophoretic deposition and characterization of chitosan/bioactive glass composite coatings on Mg alloy substrates, Electrochim. Acta 232 (2017) 456–464.

[93] G. Mani, M.D. Feldman, D. Patel, C.M. Agrawal, Coronary stents: a materials perspective, Biomaterials 28 (9) (2007) 1689–1710.

[94] Y.F. Zheng, X.N. Gu, F. Witte, Biodegradable metals, Mater. Sci. Eng., R 77 (2014) 1–34.

[95] J. Venezuela, M.S. Dargusch, The influence of alloying and fabrication techniques on the mechanical properties, biodegradability and biocompatibility of zinc: a comprehensive review, Acta Biomater. 87 (2019) 1–40.

[96] J.S. Forrester, M. Fishbein, R. Helfant, J. Fagin, A paradigm for restenosis based on cell biology: clues for the development of new preventive therapies, J. Am. Coll. Cardiol. 17 (3) (1991) 758–769.

[97] H.S. Han, S. Loffredo, I. Jun, J. Edwards, Y.C. Kim, H.K. Seok, F. Witte, D. Mantovani, S. Glyn-Jones, Current status and outlook on the clinical translation of biodegradable metals, Mater. Today 23 (2019) 57–71.

[98] C. Chen, J. Chen, W. Wu, Y. Shi, L. Jin, L. Petrini, L. Shen, G. Yuan, W. Ding, J. Ge, E.R. Edelman, F. Migliavacca, In vivo and in vitro evaluation of a biodegradable magnesium vascular stent designed by shape optimization strategy, Biomaterials 221 (2019) 119414.

[99] G. Chandra, A. Pandey, Biodegradable bone implants in orthopedic applications: a review, Biocybern. Biomed. Eng. 40 (2) (2020) 596–610.

[100] D. Zhao, F. Witte, F. Lu, J. Wang, J. Li, L. Qin, Current status on clinical applications of magnesium-based orthopaedic implants: a review from clinical translational perspective, Biomaterials 112 (2017) 287–302.

[101] T. Kraus, S.F. Fischerauer, A.C. Hänzi, P.J. Uggowitzer, J.F. Löffler, A. M. Weinberg, Magnesium alloys for temporary implants in osteosynthesis: in vivo studies of their degradation and interaction with bone, Acta Biomater. 8 (3) (2012) 1230–1238.

[102] S. Zhang, X. Zhang, C. Zhao, J. Li, Y. Song, C. Xie, H. Tao, Y. Zhang, Y. He, Y. Jiang, Y. Bian, Research on an Mg-Zn alloy as a degradable biomaterial, Acta Biomater. 6 (2) (2010) 626–640.

[103] X.N. Gu, X.H. Xie, N. Li, Y.F. Zheng, L. Qin, In vitro and in vivo studies on a Mg–Sr binary alloy system developed as a new kind of biodegradable metal, Acta Biomater. 8 (6) (2012) 2360–2374.

[104] J.L. Wang, J.K. Xu, C. Hopkins, D.H. Chow, L. Qin, Biodegradable magnesium-based implants in orthopedics-A general review and perspectives, Adv. Sci. 7 (8) (2020) 1902443.

[105] T. Kraus, F. Moszner, S. Fischerauer, M. Fiedler, E. Martinelli, J. Eichler, F. Witte, E. Willbold, M. Schinhammer, M. Meischel, P.J. Uggowitzer, J.F. Loffler, A. Weinberg, Biodegradable Fe-based alloys for use in osteosynthesis: outcome of an in vivo study after 52 weeks, Acta Biomater. 10 (7) (2014) 3346–3353.

[106] D. Pierson, J. Edick, A. Tauscher, E. Pokorney, P. Bowen, J. Gelbaugh, J. Stinson, H. Getty, C.H. Lee, J. Drelich, J. Goldman, A simplified in vivo approach for evaluating the bioabsorbable behavior of candidate stent materials, J. Biomed. Mater. Res., Part B 100 (1) (2012) 58–67.

[107] C. Xiao, L. Wang, Y. Ren, S. Sun, E. Zhang, C. Yan, Q. Liu, X. Sun, F. Shou, J. Duan, H. Wang, G. Qin, Indirectly extruded biodegradable Zn-0.05wt%Mg alloy with improved strength and ductility: in vitro and in vivo studies, J. Mater. Sci. Technol. 34 (9) (2018) 1618–1627.

[108] Y. Liu, Y. Zheng, X.H. Chen, J.A. Yang, H. Pan, D. Chen, L. Wang, J. Zhang, D. Zhu, S. Wu, K.W.K. Yeung, R.C. Zeng, Y. Han, S. Guan, Fundamental theory of biodegradable metals—definition, criteria, and design, Adv. Funct. Mater. 29 (18) (2019).

[109] H. Yang, B. Jia, Z. Zhang, X. Qu, G. Li, W. Lin, D. Zhu, K. Dai, Y. Zheng, Alloying design of biodegradable zinc as promising bone implants for load-bearing applications, Nat. Commun. 11 (1) (2020) 401.

[110] X. Wang, H.M. Lu, X.L. Li, L. Li, Y.F. Zheng, Effect of cooling rate and composition on microstructures and properties of Zn-Mg alloys, Trans. Nonferrous Metals Soc. China 17 (s1A) (2007) s122–s125.

[111] P.K. Bowen, J. Drelich, J. Goldman, Zinc exhibits ideal physiological corrosion behavior for bioabsorbable stents, Adv. Mater. 25 (18) (2013) 2577–2582.

[112] H. Tapiero, K.D. Tew, Trace elements in human physiology and pathology: zinc and metallothioneins, Biomed. Pharmacother. 57 (9) (2003) 399–411.

[113] C.T. Chasapis, A.C. Loutsidou, C.A. Spiliopoulou, M.E. Stefanidou, Zinc and human health: an update, Arch. Toxicol. 86 (4) (2012) 521–534.

[114] P.K. Bowen, E.R. Shearier, S. Zhao, R.J. Guillory 2nd, F. Zhao, J. Goldman, J. W. Drelich, Biodegradable metals for cardiovascular stents: from clinical concerns to recent Zn-alloys, Adv. Healthc. Mater. 5 (10) (2016) 1121–1140.

[115] M. Yamaguchi, Role of zinc in bone formation and bone resorption, J. Trace Elem. Exp. Med. 11 (2–3) (1998) 119–135.

[116] Y. Qiao, W. Zhang, P. Tian, F. Meng, H. Zhu, X. Jiang, X. Liu, P.K. Chu, Stimulation of bone growth following zinc incorporation into biomaterials, Biomaterials 35 (25) (2014) 6882–6897.

[117] H.J. Seo, Y.E. Cho, T. Kim, H.I. Shin, I.S. Kwun, Zinc may increase bone formation through stimulating cell proliferation, alkaline phosphatase activity and collagen synthesis in osteoblastic MC3T3-E1 cells, Nutr. Res. Pract. 4 (5) (2010) 356–361.

[118] M. Yamaguchi, R. Yamaguchi, Action of zinc on bone metabolism in rats: increases in alkaline phosphatase activity and DNA content, Biochem. Pharmacol. 35 (5) (1986) 773–777.

[119] K. Yusa, O. Yamamoto, M. Iino, H. Takano, M. Fukuda, Z. Qiao, T. Sugiyama, Eluted zinc ions stimulate osteoblast differentiation and mineralization in human dental pulp stem cells for bone tissue engineering, Arch. Oral Biol. 71 (2016) 162–169.

[120] R.M. Ortega, M.E. Quintas, P. Andrés, R.M. Martinez, A.M. López-Sobaler, A. M. Requejo, Zinc status of a group of pregnant Spanish women: effects on anthropometric data and Apgar scores of neonates, Nutr. Res. (N. Y., NY, U. S.) 19 (9) (1999) 1423–1428.

[121] B.S. Moonga, D.W. Dempster, Zinc is a potent inhibitor of osteoclastic bone resorption in vitro, J. Bone Miner. Res. 10 (3) (1995) 453–457.

[122] P.J. Little, R. Bhattacharya, A.E. Moreyra, I.L. Korichneva, Zinc and cardiovascular disease, Nutrition 26 (11–12) (2010) 1050–1057.

[123] P. Meerarani, G. Reiterer, M. Toborek, B. Hennig, Zinc modulates PPARγ signaling and activation of porcine endothelial cells, J. Nutr. 133 (10) (2003) 3058–3064.

[124] T. Kaji, Y. Fujiwara, C. Yamamoto, M. Sakamoto, H. Kozuka, Stimulation by zinc of cultured vascular endothelial cell proliferation: possible involvement of endogenous basic fibroblast growth factor, Life Sci. 55 (23) (1994) 1781–1787.

[125] M. Dardenne, Zinc and immune function, Eur. J. Clin. Nutr. 56 (4) (2002) S20–S23.

[126] W. Maret, H.H. Sandstead, Zinc requirements and the risks and benefits of zinc supplementation, J. Trace Elem. Med. Biol. 20 (1) (2006) 3–18.

[127] C.J. Frederickson, J.Y. Koh, A.I. Bush, The neurobiology of zinc in health and disease, Nat. Rev. Neurosci. 6 (6) (2005) 449–462.

[128] D. Kleiner, The effect of Zn^{2+} ions on mitochondrial electron transport, Arch. Biochem. Biophys. 165 (1) (1974) 121–125.

[129] J. Ma, N. Zhao, D. Zhu, Bioabsorbable zinc ion induced biphasic cellular responses in vascular smooth muscle cells, Sci. Rep. 6 (2016).

[130] J. Ma, N. Zhao, D. Zhu, Endothelial cellular responses to biodegradable metal zinc, ACS Biomater. Sci. Eng. 1 (11) (2015) 1174–1182.

[131] L.M. Plum, L. Rink, H. Haase, The essential toxin: impact of zinc on human health, Int. J. Environ. Res. Publ. Health 7 (4) (2010) 1342–1365.

[132] H.F. Li, X.H. Xie, Y.F. Zheng, Y. Cong, F.Y. Zhou, K.J. Qiu, X. Wang, S.H. Chen, L. Huang, L. Tian, L. Qin, Development of biodegradable Zn-1X binary alloys with nutrient alloying elements Mg, Ca and Sr, Sci. Rep. 5 (2015) 10719.

[133] G. Hercz, D.L. Andress, H.G. Nebeker, J.H. Shinaberger, D.J. Sherrard, J. W. Coburn, Reversal of aluminum-related bone disease after substituting calcium carbonate for aluminum hydroxide, Am. J. Kidney Dis. 11 (1) (1988) 70–75.
[134] S.S.A. El-Rahman, Neuropathology of aluminum toxicity in rats (glutamate and GABA impairment), Pharmacol. Res. 47 (3) (2003) 189–194.
[135] W. Yuan, D. Xia, Y. Zheng, X. Liu, S. Wu, B. Li, Y. Han, Z. Jia, D. Zhu, L. Ruan, K. Takashima, Y. Liu, Y. Zhou, Controllable biodegradation and enhanced osseointegration of ZrO_2-nanofilm coated Zn-Li alloy: in vitro and in vivo studies, Acta Biomater. 105 (2020) 290–303.
[136] Y. Su, K. Wang, J. Gao, Y. Yang, Y.X. Qin, Y. Zheng, D. Zhu, Enhanced cytocompatibility and antibacterial property of zinc phosphate coating on biodegradable zinc materials, Acta Biomater. 98 (2019) 174–185.
[137] W. Yuan, B. Li, D. Chen, D. Zhu, Y. Han, Y. Zheng, Formation mechanism, corrosion behavior, and cytocompatibility of microarc oxidation coating on absorbable high-purity zinc, ACS Biomater. Sci. Eng. 5 (2) (2018) 487–497.
[138] Y. Yang, F. Yuan, C. Gao, P. Feng, L. Xue, S. He, C. Shuai, A combined strategy to enhance the properties of Zn by laser rapid solidification and laser alloying, J. Mech. Behav. Biomed. Mater. 82 (2018) 51–60.
[139] D.A. Ribeiro, M.M. Sugui, M.A. Matsumoto, M.A. Duarte, M.E. Marques, D. M. Salvadori, Genotoxicity and cytotoxicity of mineral trioxide aggregate and regular and white Portland cements on Chinese hamster ovary (CHO) cells in vitro, Oral Surg. Oral Med. Oral Pathol. Oral Radiol. Endod. 101 (2) (2006) 258–261.
[140] N.S. Murni, M.S. Dambatta, S.K. Yeap, G.R. Froemming, H. Hermawan, Cytotoxicity evaluation of biodegradable Zn-3Mg alloy toward normal human osteoblast cells, Mater. Sci. Eng. C 49 (2015) 560–566.
[141] J. Kubásek, D. Vojtěch, E. Jablonská, I. Pospíšilová, J. Lipov, T. Ruml, Structure, mechanical characteristics and in vitro degradation, cytotoxicity, genotoxicity and mutagenicity of novel biodegradable Zn-Mg alloys, Mater. Sci. Eng. C 58 (2016) 24–35.
[142] H.R. Bakhsheshi-Rad, E. Hamzah, H.T. Low, M. Kasiri-Asgarani, S. Farahany, E. Akbari, M.H. Cho, Fabrication of biodegradable Zn-Al-Mg alloy: mechanical properties, corrosion behavior, cytotoxicity and antibacterial activities, Mater. Sci. Eng. C 73 (2017) 215–219.
[143] M.M. Alves, T. Prošek, C.F. Santos, M.F. Montemor, Evolution of the in vitro degradation of Zn–Mg alloys under simulated physiological conditions, RSC Adv. 7 (45) (2017) 28224–28233.
[144] X. Tong, D. Zhang, X. Zhang, Y. Su, Z. Shi, K. Wang, J. Lin, Y. Li, J. Lin, C. Wen, Microstructure, mechanical properties, biocompatibility, and in vitro corrosion and degradation behavior of a new Zn-5Ge alloy for biodegradable implant materials, Acta Biomater. 82 (2018) 197–204.
[145] H. Yang, X. Qu, W. Lin, D. Chen, D. Zhu, K. Dai, Y. Zheng, Enhanced osseointegration of Zn-Mg composites by tuning the release of Zn ions with sacrificial Mg-rich anode design, ACS Biomater. Sci. Eng. 5 (2) (2018) 453–467.
[146] H. Yang, X. Qu, W. Lin, C. Wang, D. Zhu, K. Dai, Y. Zheng, In vitro and in vivo studies on zinc-hydroxyapatite composites as novel biodegradable metal matrix composite for orthopedic applications, Acta Biomater. 71 (2018) 200–214.
[147] J. Lin, X. Tong, Z. Shi, D. Zhang, L. Zhang, K. Wang, A. Wei, L. Jin, J. Lin, Y. Li, C. Wen, A biodegradable Zn-1Cu-0.1Ti alloy with antibacterial properties for orthopedic applications, Acta Biomater. 106 (2020) 410–427.
[148] H.R. Bakhsheshi-Rad, E. Hamzah, H.T. Low, M.H. Cho, M. Kasiri-Asgarani, S. Farahany, A. Mostafa, M. Medraj, Thermal characteristics, mechanical properties, in vitro degradation and cytotoxicity of novel biodegradable Zn–Al–Mg and Zn–Al–Mg–xBi alloys, Acta Metall. Sin. 30 (3) (2017) 201–211.
[149] C. Shen, X. Liu, B. Fan, P. Lan, F. Zhou, X. Li, H. Wang, X. Xiao, L. Li, S. Zhao, Z. Guo, Z. Pu, Y. Zheng, Mechanical properties, in vitro degradation behavior, hemocompatibility and cytotoxicity evaluation of Zn–1.2Mg alloy for biodegradable implants, RSC Adv. 6 (89) (2016) 86410–86419.
[150] J. Lin, X. Tong, Q. Sun, Y. Luan, D. Zhang, Z. Shi, K. Wang, J. Lin, Y. Li, M. Dargusch, C. Wen, Biodegradable ternary Zn-3Ge-0.5X (X=Cu, Mg, and Fe) alloys for orthopedic applications, Acta Biomater. 115 (2020) 432–446.
[151] J. Lin, X. Tong, K. Wang, Z. Shi, Y. Li, M. Dargusch, C. Wen, Biodegradable Zn–3Cu and Zn–3Cu–0.2Ti alloys with ultrahigh ductility and antibacterial ability for orthopedic applications, J. Mater. Sci. Technol. 68 (2021) 76–90.
[152] H. Li, H. Yang, Y. Zheng, F. Zhou, K. Qiu, X. Wang, Design and characterizations of novel biodegradable ternary Zn-based alloys with IIA nutrient alloying elements Mg, Ca and Sr, Mater. Des. 83 (2015) 95–102.
[153] T. Ren, X. Gao, C. Xu, L. Yang, P. Guo, H. Liu, Y. Chen, W. Sun, Z. Song, Evaluation of as-extruded ternary Zn–Mg–Zr alloys for biomedical implantation material: in vitro and in vivo behavior, Mater. Corros. 70 (6) (2019) 1056–1070.
[154] H. Gong, K. Wang, R. Strich, J.G. Zhou, In vitro biodegradation behavior, mechanical properties, and cytotoxicity of biodegradable Zn-Mg alloy, J. Biomed. Mater. Res., Part B 103 (8) (2015) 1632–1640.
[155] E. Jablonská, D. Vojtěch, M. Fousová, J. Kubásek, J. Lipov, J. Fojt, T. Ruml, Influence of surface pre-treatment on the cytocompatibility of a novel biodegradable ZnMg alloy, Mater. Sci. Eng. C 68 (2016) 198–204.
[156] H. Guo, D. Xia, Y. Zheng, Y. Zhu, Y. Liu, Y. Zhou, A pure zinc membrane with degradability and osteogenesis promotion for guided bone regeneration: in vitro and in vivo studies, Acta Biomater. 106 (2020) 396–409.
[157] B. Jia, H. Yang, Y. Han, Z. Zhang, X. Qu, Y. Zhuang, Q. Wu, Y. Zheng, K. Dai, In vitro and in vivo studies of Zn-Mn biodegradable metals designed for orthopedic applications, Acta Biomater. 108 (2020) 358–372.
[158] D.F. Williams, On the mechanisms of biocompatibility, Biomaterials 29 (20) (2008) 2941–2953.
[159] A. Yamamoto, R. Honma, M. Sumita, Cytotoxicity evaluation of 43 metal salts using murine fibroblasts and osteoblastic cells, J. Biomed. Mater. Res. 39 (2) (1998) 331–340.
[160] L. Yang, N. Hort, D. Laipple, D. Höche, Y. Huang, K.U. Kainer, R. Willumeit, F. Feyerabend, Element distribution in the corrosion layer and cytotoxicity of alloy Mg–10Dy during in vitro biodegradation, Acta Biomater. 9 (10) (2013) 8475–8487.
[161] Y. Zheng, Bioabsorbable Metallic Stents, Functionalised Cardiovascular Stents, Elsevier, 2018, pp. 99–134.
[162] E. Mostaed, M. Sikora-Jasinska, J.W. Drelich, M. Vedani, Zinc-based alloys for degradable vascular stent applications, Acta Biomater. 71 (2018) 1–23.
[163] J. Kubásek, D. Vojtěch, Zn-based alloys as an alternative biodegradable materials, Metal 5 (2012) 23–25.
[164] H. Yang, C. Wang, C. Liu, H. Chen, Y. Wu, J. Han, Z. Jia, W. Lin, D. Zhang, W. Li, W. Yuan, H. Guo, H. Li, G. Yang, D. Kong, D. Zhu, K. Takashima, L. Ruan, J. Nie, X. Li, Y. Zheng, Evolution of the degradation mechanism of pure zinc stent in the one-year study of rabbit abdominal aorta model, Biomaterials 145 (2017) 92–105.
[165] C. Zhou, H.F. Li, Y.X. Yin, Z.Z. Shi, T. Li, X.Y. Feng, J.W. Zhang, C.X. Song, X. S. Cui, K.L. Xu, Y.W. Zhao, W.B. Hou, S.T. Lu, G. Liu, M.Q. Li, J.Y. Ma, E. Toft, A. A. Volinsky, M. Wan, X.J. Yao, C.B. Wang, K. Yao, S.K. Xu, H. Lu, S.F. Chang, J. B. Ge, L.N. Wang, H.J. Zhang, Long-term in vivo study of biodegradable Zn-Cu stent: a 2-year implantation evaluation in porcine coronary artery, Acta Biomater. 97 (2019) 657–670.
[166] C. Hehrlein, B. Schorch, N. Kress, A. Arab, C. von Zur Muhlen, C. Bode, T. Epting, J. Haberstroh, L. Mey, H. Schwarzbach, R. Kinscherf, V. Stachniss, S. Schiestel, A. Kovacs, H. Fischer, E. Nennig, Zn-alloy provides a novel platform for mechanically stable bioresorbable vascular stents, PloS One 14 (1) (2019), e0209111.
[167] H. Jin, S. Zhao, R. Guillory, P.K. Bowen, Z. Yin, A. Griebel, J. Schaffer, E.J. Earley, J. Goldman, J.W. Drelich, Novel high-strength, low-alloys Zn-Mg (<0.1wt% Mg) and their arterial biodegradation, Mater. Sci. Eng. C 84 (2018) 67–79.
[168] S. Zhao, J.M. Seitz, R. Eifler, H.J. Maier, R.J. Guillory 2nd, E.J. Earley, A. Drelich, J. Goldman, J.W. Drelich, Zn-Li alloy after extrusion and drawing: structural, mechanical characterization, and biodegradation in abdominal aorta of rat, Mater. Sci. Eng. C 76 (2017) 301–312.
[169] P.K. Bowen, J.M. Seitz, R.J. Guillory 2nd, J.P. Braykovich, S. Zhao, J. Goldman, J. W. Drelich, Evaluation of wrought Zn-Al alloys (1, 3, and 5 wt % Al) through mechanical and in vivo testing for stent applications, J. Biomed. Mater. Res., Part B 106 (1) (2018) 245–258.
[170] E. Mostaed, M. Sikora-Jasinska, A. Mostaed, S. Loffredo, A.G. Demir, B. Previtali, D. Mantovani, R. Beanland, M. Vedani, Novel Zn-based alloys for biodegradable stent applications: design, development and in vitro degradation, J. Mech. Behav. Biomed. Mater. 60 (2016) 581–602.
[171] J. Fu, Y. Su, Y.X. Qin, Y. Zheng, Y. Wang, D. Zhu, Evolution of metallic cardiovascular stent materials: a comparative study among stainless steel, magnesium and zinc, Biomaterials 230 (2020) 119641.
[172] P. Wen, M. Voshage, L. Jauer, Y. Chen, Y. Qin, R. Poprawe, J.H. Schleifenbaum, Laser additive manufacturing of Zn metal parts for biodegradable applications: processing, formation quality and mechanical properties,, Mater. Des. 155 (2018) 36–45.
[173] S. Lin, X. Ran, X. Yan, Q. Wang, J.G. Zhou, T. Hu, G. Wang, Systematical evolution on a Zn-Mg alloy potentially developed for biodegradable cardiovascular stents, J. Mater. Sci. Mater. Med. 30 (11) (2019) 122.
[174] M.S. Ardakani, E. Mostaed, M. Sikora-Jasinska, S.L. Kampe, J.W. Drelich, The effects of alloying with Cu and Mn and thermal treatments on the mechanical instability of Zn-0.05Mg alloy, Mater. Sci. Eng., A (2020) 770.
[175] Y. Dai, Y. Zhang, H. Liu, H. Fang, D. Li, X. Xu, Y. Yan, L. Chen, Y. Lu, K. Yu, Mechanical strengthening mechanism of Zn-Li alloy and its mini tube as potential absorbable stent material, Mater. Lett. 235 (2019) 220–223.
[176] S. Zhao, C.T. McNamara, P.K. Bowen, N. Verhun, J.P. Braykovich, J. Goldman, J. W. Drelich, Structural characteristics and in vitro biodegradation of a novel Zn-Li alloy prepared by induction melting and hot rolling, Metall. Mater. Trans. 48 (3) (2017) 1204–1215.
[177] Z. Tang, J. Niu, H. Huang, H. Zhang, J. Pei, J. Ou, G. Yuan, Potential biodegradable Zn-Cu binary alloys developed for cardiovascular implant applications, J. Mech. Behav. Biomed. Mater. 72 (2017) 182–191.
[178] R. Yue, J. Niu, Y. Li, G. Ke, H. Huang, J. Pei, W. Ding, G. Yuan, In vitro cytocompatibility, hemocompatibility and antibacterial properties of biodegradable Zn-Cu-Fe alloys for cardiovascular stents applications, Mater. Sci. Eng. C 113 (2020) 111007.
[179] R. Yue, H. Huang, G. Ke, H. Zhang, J. Pei, G. Xue, G. Yuan, Microstructure, mechanical properties and in vitro degradation behavior of novel Zn-Cu-Fe alloys, Mater. Char. 134 (2017) 114–122.
[180] J. Niu, Z. Tang, H. Huang, J. Pei, H. Zhang, G. Yuan, W. Ding, Research on a Zn-Cu alloy as a biodegradable material for potential vascular stents application, Mater. Sci. Eng. C 69 (2016) 407–413.
[181] S. Sun, Y. Ren, L. Wang, B. Yang, H. Li, G. Qin, Abnormal effect of Mn addition on the mechanical properties of as-extruded Zn alloys, Mater. Sci. Eng., A 701 (2017) 129–133.
[182] M. Sikora-Jasinska, E. Mostaed, A. Mostaed, R. Beanland, D. Mantovani, M. Vedani, Fabrication, mechanical properties and in vitro degradation behavior of newly developed ZnAg alloys for degradable implant applications, Mater. Sci. Eng. C 77 (2017) 1170–1181.
[183] S. Lin, X. Ran, X. Yan, W. Yan, Q. Wang, T. Yin, J.G. Zhou, T. Hu, G. Wang, Corrosion behavior and biocompatibility evaluation of a novel zinc-based alloy

stent in rabbit carotid artery model, J. Biomed. Mater. Res., Part B 107 (6) (2019) 1814–1823.
[184] S. Lin, Q. Wang, X. Yan, X. Ran, L. Wang, J.G. Zhou, T. Hu, G. Wang, Mechanical properties, degradation behaviors and biocompatibility evaluation of a biodegradable Zn-Mg-Cu alloy for cardiovascular implants, Mater. Lett. 234 (2019) 294–297.
[185] C. Chen, R. Yue, J. Zhang, H. Huang, J. Niu, G. Yuan, Biodegradable Zn-1.5Cu-1.5Ag alloy with anti-aging ability and strain hardening behavior for cardiovascular stents, Mater. Sci. Eng. C 116 (2020) 111172.
[186] Z. Tang, H. Huang, J. Niu, L. Zhang, H. Zhang, J. Pei, J. Tan, G. Yuan, Design and characterizations of novel biodegradable Zn-Cu-Mg alloys for potential biodegradable implants, Mater. Des. 117 (2017) 84–94.
[187] Z.Z. Shi, J. Yu, X.F. Liu, L.N. Wang, Fabrication and characterization of novel biodegradable Zn-Mn-Cu alloys, J. Mater. Sci. Technol. 34 (6) (2018) 1008–1015.
[188] R.J. Guillory, A.A. Oliver, E.K. Davis, E.J. Earley, J.W. Drelich, J. Goldman, Preclinical in vivo evaluation and screening of zinc-based degradable metals for endovascular stents, JOM 71 (4) (2019) 1436–1446.
[189] P.K. Bowen, R.J. Guillory II, E.R. Shearier, J.M. Seitz, J. Drelich, M. Bocks, F. Zhao, J. Goldman, Metallic zinc exhibits optimal biocompatibility for bioabsorbable endovascular stents, Mater. Sci. Eng. C 56 (2015) 467–472.
[190] L. Zhang, X. Tong, J. Lin, Y. Li, C. Wen, Enhanced corrosion resistance via phosphate conversion coating on pure Zn for medical applications, Corrosion Sci. 169 (2020).
[191] Y. Zhuang, Q. Liu, G. Jia, H. Li, G. Yuan, H. Yu, A biomimetic zinc alloy scaffold coated with brushite for enhanced cranial bone regeneration, ACS Biomater. Sci. Eng. 7 (3) (2021) 893–903.
[192] G. Katarivas Levy, A. Kafri, Y. Ventura, A. Leon, R. Vago, J. Goldman, E. Aghion, Surface stabilization treatment enhances initial cell viability and adhesion for biodegradable zinc alloys, Mater. Lett. 248 (2019) 130–133.
[193] F. Peng, Y. Lin, D. Zhang, Q. Ruan, K. Tang, M. Li, X. Liu, P.K. Chu, Y. Zhang, Corrosion behavior and biocompatibility of diamond-like carbon-coated zinc: an in vitro study, ACS Omega 6 (14) (2021) 9843–9851.
[194] P. Li, J. Qian, W. Zhang, C. Schille, E. Schweizer, A. Heiss, U.E. Klotz, L. Scheideler, G. Wan, J. Geis-Gerstorfer, Improved biodegradability of zinc and its alloys by sandblasting treatment, Surf. Coating. Technol. 405 (2021).
[195] L. Herschke, J. Rottstegge, I. Lieberwirth, G. Wegner, Zinc phosphate as versatile material for potential biomedical applications Part 1, J. Mater. Sci. Mater. Med. 17 (1) (2006) 81–94.
[196] L. Herschke, I. Lieberwirth, G. Wegner, Zinc phosphate as versatile material for potential biomedical applications Part II, J. Mater. Sci. Mater. Med. 17 (1) (2006) 95–104.
[197] S.M.A. Shibli, A.C. Jayalekshmi, Development of phosphate inter layered hydroxyapatite coating for stainless steel implants, Appl. Surf. Sci. 254 (13) (2008) 4103–4110.
[198] Q. Zhang, Y. Leng, Electrochemical activation of titanium for biomimetic coating of calcium phosphate, Biomaterials 26 (18) (2005) 3853–3859.
[199] H.M. Wong, K.W.K. Yeung, K.O. Lam, V. Tam, P.K. Chu, K.D.K. Luk, K.M. C. Cheung, A biodegradable polymer-based coating to control the performance of magnesium alloy orthopaedic implants, Biomaterials 31 (8) (2010) 2084–2096.
[200] G.K. Soujanya, T. Hanas, V.Y. Chakrapani, B.R. Sunil, T.S.S. Kumar, Electrospun nanofibrous polymer coated magnesium alloy for biodegradable implant applications, Procedia Mater. Sci. 5 (2014) 817–823.
[201] A. Abdal-hay, N.A.M. Barakat, J.K. Lim, Hydroxyapatite-doped poly(lactic acid) porous film coating for enhanced bioactivity and corrosion behavior of AZ31 Mg alloy for orthopedic applications, Ceram. Int. 39 (1) (2013) 183–195.
[202] Z. Hu, Q. Chen, Z. Li, Y. Yu, L.M. Peng, Large-scale and rapid synthesis of ultralong ZnO nanowire films via anodization, J. Phys. Chem. C 114 (2) (2010) 881–889.
[203] S.J. Kim, J. Choi, Self-assembled arrays of ZnO stripes by anodization, Electrochem. Commun. 10 (1) (2008) 175–179.
[204] J. Zhao, X. Wang, J. Liu, Y. Meng, X. Xu, C. Tang, Controllable growth of zinc oxide nanosheets and sunflower structures by anodization method, Mater. Chem. Phys. 126 (3) (2011) 555–559.
[205] A.Y. Faid, N.K. Allam, Stable solar-driven water splitting by anodic ZnO nanotubular semiconducting photoanodes, RSC Adv. 6 (83) (2016) 80221–80225.
[206] S. Gilani, M. Ghorbanpour, A. Parchehbaf Jadid, Antibacterial activity of ZnO films prepared by anodizing, J. Nanostruct. Chem. 6 (2) (2016) 183–189.
[207] H. Lyu, Z. He, Y.K. Chan, X. He, Y. Yu, Y. Deng, Hierarchical ZnO nanotube/graphene oxide nanostructures endow pure Zn implant with synergistic bactericidal activity and osteogenicity, Ind. Eng. Chem. Res. 58 (42) (2019) 19377–19385.
[208] H. Tang, Y. Gao, Preparation and characterization of hydroxyapatite containing coating on AZ31 magnesium alloy by micro-arc oxidation, J. Alloys Compd. 688 (2016) 699–708.
[209] C. Yu, L.Y. Cui, Y.F. Zhou, Z.Z. Han, X.B. Chen, R.C. Zeng, Y.H. Zou, S.Q. Li, F. Zhang, E.H. Han, S.K. Guan, Self-degradation of micro-arc oxidation/chitosan composite coating on Mg-4Li-1Ca alloy, Surf. Coating. Technol. 344 (2018) 1–11.
[210] Z.Y. Li, Z.B. Cai, Y. Cui, J.H. Liu, M.H. Zhu, Effect of oxidation time on the impact wear of micro-arc oxidation coating on aluminum alloy, Wear 426–427 (2019) 285–295.
[211] T. Wei, F. Yan, J. Tian, Characterization and wear- and corrosion-resistance of microarc oxidation ceramic coatings on aluminum alloy, J. Alloys Compd. 389 (1–2) (2005) 169–176.
[212] G. Li, H. Cao, W. Zhang, X. Ding, G. Yang, Y. Qiao, X. Liu, X. Jiang, Enhanced osseointegration of hierarchical micro/nanotopographic titanium fabricated by microarc oxidation and electrochemical treatment, ACS Appl. Mater. Interfaces 8 (6) (2016) 3840–3852.
[213] L. Bai, Z. Du, J. Du, W. Yao, J. Zhang, Z. Weng, S. Liu, Y. Zhao, Y. Liu, X. Zhang, X. Huang, X. Yao, R. Crawford, R. Hang, D. Huang, B. Tang, Y. Xiao, A multifaceted coating on titanium dictates osteoimmunomodulation and osteo/angio-genesis towards ameliorative osseointegration, Biomaterials 162 (2018) 154–169.
[214] D.M. Hausmann, E. Kim, J. Becker, R.G. Gordon, Atomic layer deposition of hafnium and zirconium oxides using metal amide precursors, Chem. Mater. 14 (10) (2002) 4350–4358.
[215] S.M. George, Atomic layer deposition: an overview, Chem. Rev. 110 (1) (2010) 111–131.
[216] Q. Yang, W. Yuan, X. Liu, Y. Zheng, Z. Cui, X. Yang, H. Pan, S. Wu, Atomic layer deposited ZrO_2 nanofilm on Mg-Sr alloy for enhanced corrosion resistance and biocompatibility, Acta Biomater. 58 (2017) 515–526.
[217] W. Jin, H. Zhou, J. Li, Q. Ruan, J. Li, X. Peng, W. Li, P.K. Chu, Zirconium-based nanostructured coating on the Mg-4Y-3RE alloy for corrosion retardation, Chem. Phys. Lett. 756 (2020) 137824.
[218] E. Bolbasov, P. Maryin, K. Stankevich, A. Kozelskaya, E. Shesterikov, Y. I. Khodyrevskaya, M. Nasonova, D. Shishkova, Y.A. Kudryavtseva, Y. Anissimov, Surface modification of electrospun poly-(L-lactic) acid scaffolds by reactive magnetron sputtering, Colloids Surf. B Biointerfaces 162 (2018) 43–51.
[219] C.Y. Guo, A.T.H. Tang, J.P. Matinlinna, Insights into surface treatment methods of titanium dental implants, J. Adhes. Sci. Technol. 26 (1–3) (2012) 189–205.
[220] C.Y. Guo, J.P. Matinlinna, A.T.H. Tang, A novel effect of sandblasting on titanium surface: static charge generation, J. Adhes. Sci. Technol. 26 (23) (2012) 2603–2613.
[221] E.R. Shearier, P.K. Bowen, W. He, A. Drelich, J. Drelich, J. Goldman, F. Zhao, In vitro cytotoxicity, adhesion, and proliferation of human vascular cells exposed to zinc, ACS Biomater. Sci. Eng. 2 (4) (2016) 634–642.
[222] A.A. Shomali, R.J. Guillory, D. Seguin, J. Goldman, J.W. Drelich, Effect of PLLA coating on corrosion and biocompatibility of zinc in vascular environment, Surf. Innovations 5 (4) (2017) 211–220.
[223] A.J. Drelich, P.K. Bowen, L. LaLonde, J. Goldman, J.W. Drelich, Importance of oxide film in endovascular biodegradable zinc stents, Surf. Innovations 4 (3) (2016) 133–140.
[224] Y. Sheng, H. Zhou, Z. Li, L. Chen, X. Wang, X. Zhao, W. Li, Improved blood compatibility and cyto-compatibility of Zn-1Mg via plasma electrolytic oxidation, Materialia 5 (2019).
[225] Y. Sheng, J. Yang, R. Hou, L. Chen, J. Xu, H. Liu, X. Zhao, X. Wang, R. Zeng, W. Li, Y. Xie, Improved biocompatibility and degradation behavior of biodegradable Zn-1Mg by grafting zwitterionic phosphorylcholine chitosan (PCCs) coating on silane pre-modified surface, Appl. Surf. Sci. 527 (2020).
[226] R.J. Guillory 2nd, M. Sikora-Jasinska, J.W. Drelich, J. Goldman, In vitro corrosion and in vivo response to zinc implants with electropolished and anodized surfaces, ACS Appl. Mater. Interfaces 11 (22) (2019) 19884–19893.
[227] I. Antoniac, F. Miculescu, C. Cotrut, A. Ficai, J.V. Rau, E. Grosu, A. Antoniac, C. Tecu, I. Cristescu, Controlling the degradation rate of biodegradable Mg–Zn-Mn alloys for orthopedic applications by electrophoretic deposition of hydroxyapatite coating, Materials 13 (2) (2020) 263.
[228] B. Istrate, J.V. Rau, C. Munteanu, I.V. Antoniac, V. Saceleanu, Properties and in vitro assessment of ZrO_2-based coatings obtained by atmospheric plasma jet spraying on biodegradable Mg-Ca and Mg-Ca-Zr alloys, Ceram. Int. 46 (10) (2020) 15897–15906.
[229] H. Wang, Y. Zheng, C. Jiang, Y. Li, Y. Fu, In vitro corrosion behavior and cytocompatibility of pure Fe implanted with Ta, Surf. Coating. Technol. 320 (2017) 201–205.
[230] T. Huang, Y. Cheng, Y. Zheng, In vitro studies on silver implanted pure iron by metal vapor vacuum arc technique, Colloids Surf., B 142 (2016) 20–29.
[231] S.N. Nayab, F.H. Jones, I. Olsen, Effects of calcium ion-implantation of titanium on bone cell function in vitro, J. Biomed. Mater. Res. 83 (2) (2007) 296–302.
[232] L.Y. Li, L.Y. Cui, R.C. Zeng, S.Q. Li, X.B. Chen, Y. Zheng, M.B. Kannan, Advances in functionalized polymer coatings on biodegradable magnesium alloys - a review, Acta Biomater. 79 (2018) 23–36.
[233] W.J. Lin, D.Y. Zhang, G. Zhang, H.T. Sun, H.P. Qi, L.P. Chen, Z.Q. Liu, R.L. Gao, W. Zheng, Design and characterization of a novel biocorrodible iron-based drug-eluting coronary scaffold, Mater. Des. 91 (2016) 72–79.
[234] A.H. Yusop, N.M. Daud, H. Nur, M.R. Kadir, H. Hermawan, Controlling the degradation kinetics of porous iron by poly(lactic-co-glycolic acid) infiltration for use as temporary medical implants, Sci. Rep. 5 (2015) 11194.
[235] X. Meng, M. Duan, L. Luo, D. Zhan, B. Jin, Y. Jin, X.X. Rao, Y. Liu, J. Lu, The deformation behavior of AZ31 Mg alloy with surface mechanical attrition treatment, Mater. Sci. Eng., A 707 (2017) 636–646.
[236] N. Li, Y.D. Li, Y.X. Li, Y.H. Wu, Y.F. Zheng, Y. Han, Effect of surface mechanical attrition treatment on biodegradable Mg–1Ca alloy, Mater. Sci. Eng. C 35 (2014) 314–321.
[237] S. Bagherifard, M.F. Molla, D. Kajanek, R. Donnini, B. Hadzima, M. Guagliano, Accelerated biodegradation and improved mechanical performance of pure iron through surface grain refinement, Acta Biomater. 98 (2019) 88–102.
[238] P. Xiong, Z. Jia, W. Zhou, J. Yan, P. Wang, W. Yuan, Y. Li, Y. Cheng, Z. Guan, Y. Zheng, Osteogenic and pH stimuli-responsive self-healing coating on biomedical Mg-1Ca alloy, Acta Biomater. 92 (2019) 336–350.
[239] S. Heise, S. Virtanen, A.R. Boccaccini, Tackling Mg alloy corrosion by natural polymer coatings-A review, J. Biomed. Mater. Res. 104 (10) (2016) 2628–2641.
[240] X. Luo, X.T. Cui, Electrochemical deposition of conducting polymer coatings on magnesium surfaces in ionic liquid, Acta Biomater. 7 (1) (2011) 441–446.

[241] S. Agarwal, M. Riffault, D. Hoey, B. Duffy, J. Curtin, S. Jaiswal, Biomimetic hyaluronic acid-lysozyme composite coating on AZ31 Mg alloy with combined antibacterial and osteoinductive activities, ACS Biomater. Sci. Eng. 3 (12) (2017) 3244–3253.
[242] J. Jeong, J.H. Kim, J.H. Shim, N.S. Hwang, C.Y. Heo, Bioactive calcium phosphate materials and applications in bone regeneration, Biomater. Res. 23 (2019) 4.
[243] L.Y. Cui, G.B. Wei, Z.Z. Han, R.C. Zeng, L. Wang, Y.H. Zou, S.Q. Li, D.K. Xu, S. K. Guan, In vitro corrosion resistance and antibacterial performance of novel tin dioxide-doped calcium phosphate coating on degradable Mg-1Li-1Ca alloy, J. Mater. Sci. Technol. 35 (3) (2019) 254–265.
[244] D. Xiao, J. Zhang, C. Zhang, D. Barbieri, H. Yuan, L. Moroni, G. Feng, The role of calcium phosphate surface structure in osteogenesis and the mechanisms involved, Acta Biomater. 106 (2020) 22–33.
[245] S. Shadanbaz, G.J. Dias, Calcium phosphate coatings on magnesium alloys for biomedical applications: a review, Acta Biomater. 8 (1) (2012) 20–30.
[246] X. Guan, M. Xiong, F. Zeng, B. Xu, L. Yang, H. Guo, J. Niu, J. Zhang, C. Chen, J. Pei, H. Huang, G. Yuan, Enhancement of osteogenesis and biodegradation control by brushite coating on Mg-Nd-Zn-Zr alloy for mandibular bone repair, ACS Appl. Mater. Interfaces 6 (23) (2014) 21525–21533.
[247] I.V. Antoniac, M. Filipescu, K. Barbaro, A. Bonciu, R. Birjega, C.M. Cotrut, E. Galvano, M. Fosca, I.V. Fadeeva, G. Vadalà, Iron ion-doped tricalcium phosphate coatings improve the properties of biodegradable magnesium alloys for biomedical implant application, Adv. Mater. Interfaces 7 (16) (2020) 2000531.
[248] J.V. Rau, I. Antoniac, M. Filipescu, C. Cotrut, M. Fosca, L.C. Nistor, R. Birjega, M. Dinescu, Hydroxyapatite coatings on Mg-Ca alloy prepared by pulsed laser deposition: properties and corrosion resistance in simulated body fluid, Ceram. Int. 44 (14) (2018) 16678–16687.
[249] B. Niu, P. Shi, D. Wei, E. Shanshan, Q. Li, Y. Chen, Effects of sintering temperature on the corrosion behavior of AZ31 alloy with Ca–P sol–gel coating, J. Alloys Compd. 665 (2016) 435–442.
[250] H.X. Wang, S.K. Guan, X. Wang, C.X. Ren, L.G. Wang, In vitro degradation and mechanical integrity of Mg–Zn–Ca alloy coated with Ca-deficient hydroxyapatite by the pulse electrodeposition process, Acta Biomater. 6 (5) (2010) 1743–1748.
[251] A. Ali, F. Iqbal, A. Ahmad, F. Ikram, A. Nawaz, A.A. Chaudhry, S.A. Siddiqi, I. Rehman, Hydrothermal deposition of high strength calcium phosphate coatings on magnesium alloy for biomedical applications, Surf. Coating. Technol. 357 (2019) 716–727.
[252] F. Sima, G. Socol, E. Axente, I.N. Mihailescu, L. Zdrentu, S.M. Petrescu, I. Mayer, Biocompatible and bioactive coatings of Mn^{2+}-doped β-tricalcium phosphate synthesized by pulsed laser deposition, Appl. Surf. Sci. 254 (4) (2007) 1155–1159.
[253] J. Li, K. Zhang, N. Huang, Engineering cardiovascular implant surfaces to create a vascular endothelial growth microenvironment, Biotechnol. J. 12 (12) (2017).
[254] D.I. Axel, W. Kunert, C. Göggelmann, M. Oberhoff, C. Herdeg, A. Küttner, D. H. Wild, B.R. Brehm, R. Riessen, G. Köveker, Paclitaxel inhibits arterial smooth muscle cell proliferation and migration in vitro and in vivo using local drug delivery, Circulation 96 (2) (1997) 636–645.
[255] J.M. Daniel, J. Dutzmann, H. Brunsch, J. Bauersachs, R. Braun-Dullaeus, D. G. Sedding, Systemic application of sirolimus prevents neointima formation not via a direct anti-proliferative effect but via its anti-inflammatory properties, Int. J. Cardiol. 238 (2017) 79–91.
[256] T. Schachner, Y. Zou, A. Oberhuber, A. Tzankov, T. Mairinger, G. Laufer, J. O. Bonatti, Local application of rapamycin inhibits neointimal hyperplasia in experimental vein grafts, Ann. Thorac. Surg. 77 (5) (2004) 1580–1585.
[257] Q. Javed, N. Swanson, H. Vohra, H. Thurston, A.H. Gershlick, Tumor necrosis factor-alpha antibody eluting stents reduce vascular smooth muscle cell proliferation in saphenous vein organ culture, Exp. Mol. Pathol. 73 (2) (2002) 104–111.
[258] A. Farb, P.F. Heller, S. Shroff, L. Cheng, F.D. Kolodgie, A.J. Carter, D.S. Scott, J. Froehlich, R. Virmani, Pathological analysis of local delivery of paclitaxel via a polymer-coated stent, Circulation 104 (4) (2001) 473–479.
[259] Y. Shi, L. Zhang, J. Chen, J. Zhang, F. Yuan, L. Shen, C. Chen, J. Pei, Z. Li, J. Tan, G. Yuan, In vitro and in vivo degradation of rapamycin-eluting Mg-Nd-Zn-Zr alloy stents in porcine coronary arteries, Mater. Sci. Eng. C 80 (2017) 1–6.
[260] P. Ramadugu, K. Latha Alikatte, N. Dhudipala, V. Bommasane, Review on nitric oxide, carbon monoxide and antisense based therapy towards treatment of restenosis, J. Bioequivalence Bioavailab. 8 (2) (2016).
[261] F. Zhang, Q. Zhang, X. Li, N. Huang, X. Zhao, Z. Yang, Mussel-inspired dopamine-Cu(II) coatings for sustained in situ generation of nitric oxide for prevention of stent thrombosis and restenosis, Biomaterials 194 (2019) 117–129.
[262] E. Young, The anti-inflammatory effects of heparin and related compounds, Thromb. Res. 122 (6) (2008) 743–752.
[263] S.H. Ye, C.A. Johnson Jr., J.R. Woolley, H. Murata, L.J. Gamble, K. Ishihara, W. R. Wagner, Simple surface modification of a titanium alloy with silanated zwitterionic phosphorylcholine or sulfobetaine modifiers to reduce thrombogenicity, Colloids Surf., B 79 (2) (2010) 357–364.
[264] M. Amiji, H. Park, K. Park, Study on the prevention of surface-induced platelet activation by albumin coating, J. Biomater. Sci. Polym. Ed. 3 (5) (1992) 375–388.
[265] S.J. Lee, H.H. Jo, K.S. Lim, D. Lim, S. Lee, J.H. Lee, W.D. Kim, M.H. Jeong, J. Y. Lim, I.K. Kwon, Y. Jung, J.K. Park, S.A. Park, Heparin coating on 3D printed poly (l-lactic acid) biodegradable cardiovascular stent via mild surface modification approach for coronary artery implantation, Chem. Eng. J. (2019) 378.
[266] S. Zhu, N. Huang, L. Xu, Y. Zhang, H. Liu, Y. Lei, H. Sun, Y. Yao, Biocompatibility of Fe–O films synthesized by plasma immersion ion implantation and deposition, Surf. Coating. Technol. 203 (10–11) (2009) 1523–1529.
[267] S. Zhu, N. Huang, H. Shu, Y. Wu, L. Xu, Corrosion resistance and blood compatibility of lanthanum ion implanted pure iron by MEVVA, Appl. Surf. Sci. 256 (1) (2009) 99–104.
[268] Y. Sugita, Y. Suzuki, K. Someya, A. Ogawa, H. Furuhata, S. Miyoshi, T. Motomura, H. Miyamoto, S. Igo, Y. Nose, Experimental evaluation of a new antithrombogenic stent using ion beam surface modification, Artif. Organs 33 (6) (2009) 456–463.
[269] S. Pacharra, R. Ortiz, S. McMahon, W. Wang, R. Viebahn, J. Salber, I. Quintana, Surface patterning of a novel PEG-functionalized poly-l-lactide polymer to improve its biocompatibility: applications to bioresorbable vascular stents, J. Biomed. Mater. Res., Part B 107 (3) (2019) 624–634.
[270] K.B. Vartanian, S.J. Kirkpatrick, S.R. Hanson, M.T. Hinds, Endothelial cell cytoskeletal alignment independent of fluid shear stress on micropatterned surfaces, Biochem. Biophys. Res. Commun. 371 (4) (2008) 787–792.
[271] C. Liang, Y. Hu, H. Wang, D. Xia, Q. Li, J. Zhang, J. Yang, B. Li, H. Li, D. Han, M. Dong, Biomimetic cardiovascular stents for in vivo re-endothelialization, Biomaterials 103 (2016) 170–182.
[272] L. Chen, J. Li, S. Wang, S. Zhu, C. Zhu, B. Zheng, G. Yang, S. Guan, Surface modification of the biodegradable cardiovascular stent material Mg–Zn–Y–Nd alloy via conjugating REDV peptide for better endothelialization, J. Mater. Res. 33 (23) (2018) 4123–4133.
[273] Y.M. Shin, Y.B. Lee, S.J. Kim, J.K. Kang, J.C. Park, W. Jang, H. Shin, Mussel-inspired immobilization of vascular endothelial growth factor (VEGF) for enhanced endothelialization of vascular grafts, Biomacromolecules 13 (7) (2012) 2020–2028.
[274] Z. Yang, Q. Tu, J. Wang, N. Huang, The role of heparin binding surfaces in the direction of endothelial and smooth muscle cell fate and re-endothelialization, Biomaterials 33 (28) (2012) 6615–6625.
[275] Q. Lin, X. Ding, F. Qiu, X. Song, G. Fu, J. Ji, In situ endothelialization of intravascular stents coated with an anti-CD34 antibody functionalized heparin-collagen multilayer, Biomaterials 31 (14) (2010) 4017–4025.
[276] J. Aoki, P.W. Serruys, H. van Beusekom, A.T. Ong, E.P. McFadden, G. Sianos, W. J. van der Giessen, E. Regar, P.J. de Feyter, H.R. Davis, S. Rowland, M.J. Kutryk, Endothelial progenitor cell capture by stents coated with antibody against CD34: the HEALING-FIM (healthy endothelial accelerated lining inhibits neointimal growth-first in man) registry, J. Am. Coll. Cardiol. 45 (10) (2005) 1574–1579.